Research in Globalization 7 (2023) 100159

Contents lists available at ScienceDirect

Research in Globalization

journal homepage: www.sciencedirect.com/journal/research-in-globalization

Euro area inflation and a new measure of core inflation

Claudio Morana [a,*]

[a] University of Milano-Bicocca, Center for European Studies (CefES-DEMS), Rimini Centre for Economic Analysis (RCEA-Europe ETS; RCEA-HQ), Center for Research on Pensions and Welfare Policies (CeRP), Italy

ARTICLE INFO

Keywords:
Headline inflation
Core inflation
Russia's war in Ukraine
COVID-19 pandemic
Sovereign debt crisis
Subprime financial crisis
Dot-com bubble
Euro area
ECB monetary policy
Trend-cycle decomposition

ABSTRACT

This paper introduces a new decomposition of euro area headline inflation into core, cyclical, and residual components. Our new core inflation measure, the *structural core inflation* rate, is the expected headline inflation, conditional to medium to long-term demand and supply-side developments. It shows smoothness and trending properties, economic content, and forecasting ability for headline inflation and other available core inflation measures routinely used at the ECB for internal or external communication. Hence, it carries additional helpful information for policy-making decisions. Concerning recent developments, all the inflation components contributed to its post-pandemic upsurge. Since mid-2021, core inflation has been downward, landing at about 3% in 2022. Cyclical and residual inflation-associated with idiosyncratic supply chains, energy markets, and geopolitical tensions- are currently the major threats to price stability. While some cyclical stabilization is ongoing, a stagflation scenario cum weakening overall financial conditions might emerge. A pressing issue for ECB monetary policy will be to face -mostly supply-side- inflationary pressure without triggering a financial crisis.

1. Introduction

One practical implication of central banks' medium-term orientation and lags in the transmission mechanism is that monetary policy should not react to transient headline inflation developments. Moreover, within an inflation forecast targeting approach, a central bank should adjust the policy instrument so that the inflation forecast is about the inflation target (Svensson, 1997). This requires disentangling persistent or core (trend) and non-persistent headline inflation movements.

Since the 1970s, various approaches to core inflation measurement have been proposed. The seminal approach eliminates seasonal fluctuations and goods whose price fluctuations are highly erratic, i.e., the Ex. Food & Energy inflation rate (Eckstein, 1981; Gordon, 1975; Blinder, 1982). Since the early 1990s, two new lines of research on core inflation have developed, i.e., the cross-sectional approach of Bryan and Cecchetti (1994) and the time-series approach of Quah and Vahey (1995). The former case estimates persistent inflation by limited influence estimators, such as the trimmed mean and weighted median, which are robust to extreme and erratic price movements and measure more accurately the central tendency of the price change distribution than the mean. The latter case relates persistent inflation with the medium- to long-term output-neutral shock -within a bivariate SVAR model of output and inflation. Several other contributions have then followed within these lines of research, such as the long-run inflation forecast (Bagliano & Morana, 1999; Bagliano & Morana, 2003; Bagliano, Golinelli, & Morana, 2002; see also Martens, 2016; Chan, Clark, & Koop, 2018; Hasenzagl, Pellegrino, Reichlin, & Ricco, 2022; Kishor & Koenig, 2022), the common persistent component in inflation and excess nominal money growth (Morana, 2002; Morana, 2007), the Supercore inflation rate (Fröhling & Lommatzsch, 2011; Ehrmann, Ferrucci, Lenza, & O'Brien, 2018), the Persistent and Common Component of Inflation (Cristadoro, Forni, Reichlin, & Veronese, 2005; Bańbura & Bobeica, 2020). See the Online Appendix for a detailed account of the literature.

In addition to various limited influence estimators and exclusion measures, the ECB and other central banks use some latter measures as internal assessment tools. Relying on multiple measures of core inflation in monitoring underlying headline inflation developments grants some robustness to monetary policy tuning against the uncertainty arising from trend inflation unobservability. Understanding the origins of inflation is also essential in this respect. In the euro area, the pandemic shock was multi-dimensional (Nickel, Koester, & Lis, 2022). It involved supply restrictions triggered by lockdowns and containment measures

* Corresponding author at: Università di Milano – Bicocca, Dipartimento di Economia, Metodi Quantitativi e Strategie di Impresa, Piazza dell'Ateneo Nuovo 1, 20126 Milano, Italy.
E-mail address: claudio.morana@unimib.it.

https://doi.org/10.1016/j.resglo.2023.100159

Available online 18 October 2023

(negative aggregate supply shock), counteracted by a significant, expansionary monetary and fiscal policy response (positive aggregate demand shock). Since February 2022, Russia's war in Ukraine has strengthened supply-side inflationary pressure through rising energy and non-energy commodity prices. How large has been the entrenchment of inflationary pressure in the core inflation rate is an open question. Uncertainty about the actual level of the underlying inflation rate appears to have increased in the most recent period, as shown by the sizable divergence of the various internal ECB core inflation measures from the official ECB core inflation rate (see Fig. 1). An accurate assessment of future inflation dynamics is a "diagnostic challenge". It requires a comprehensive macro-financial framework in light of the interconnections between economic activity, financial conditions, and inflation dynamics (Lane, 2022).

Against this background, this paper investigates the drivers of euro area inflation since its foundation in 1999, focusing on current developments. The analysis exploits an innovative multivariate decomposition of headline inflation into a core or medium to long-term component, a cyclical (non-core) short-term component, and a residual part related to other short-lived factors. Following Morana (2021), estimation and disentangling are performed within a medium-scale euro area model, counting twenty-eight macro-financial variables. It exploits a much more extensive information set than in previous small-scale structural common trends models (Bagliano & Morana, 1999; Bagliano & Morana, 2003; Hasenzagl et al., 2022). Also, differently from earlier contributions in the literature, it is agnostic concerning the statistical properties of core inflation's DGP and, therefore, robust to trend inflation specification.

The new core inflation measure, i.e., the *structural core inflation rate* (*STC*), bears the interpretation of expected headline inflation, conditional to medium to long-term demand and supply-side drivers of underlying inflation. Friedman's insights from the quantity theory of money and Eckstein's insights about steady-state inflation and agents' price inflation expectations yield its theoretical grounding. In light of its definition and construction, it fits with the expected inflation rate component in a textbook Phillip's curve. By uncovering and disentangling underlying inflation economic drivers, the structural core inflation rate yields additional insights on the origins of headline inflation valuable to policy analysis.

We find that *STC* forecasts and acts as a trend for headline inflation and other available ECB core inflation measures, such as the Supercore, the Persistent Common Component of Inflation, the Trimmed Mean and Weighted Median, and the Ex-Food and Energy inflation rate. Hence, it might be useful as an additional internal tool of inflation analysis for monetary policy, carrying information on the origins of trend inflationary pressure. Our measure of cyclical inflation also carries valuable information on expected headline inflation, conditional to short-term demand and supply-side developments.

Within our decomposition framework, we can track the evolution of euro area inflation since its inception. Concerning recent developments, core inflation slightly declined during the pandemic recession due to demand-side core inflation partially offsetting the disinflationary supply-side impulse. The offsetting continued in the post-recession period as demand-side core inflation tamed the surge in the supply-side core part. The core inflation rate has decreased since mid-2021, reaching 3% in 2022. Demand-side factors largely accounted for the cyclical inflation contraction during the pandemic recession and exercised an inflationary effect afterward. Cyclical supply-side factors contributed to a prolonged disinflationary environment throughout early 2021 and reinflation only after that. The cyclical and residual inflation components largely account for the post-2020 inflation upsurge, and cyclical headline inflation appears to have lost momentum. Differently, residual inflation is a constant source of inflationary pressure in the euro area due to unfavorable supply chain and energy price developments and further ongoing geopolitical tensions.

Notwithstanding the inflationary pressure, ECB monetary policy has successfully mitigated the rise in core inflation. Some cyclical stabilization might also be ongoing. Yet cyclical and residual inflation remain the most prominent threats to price stability within a likely scenario of weakening overall financial conditions and stagflation. A pressing issue for ECB monetary policy will be to face -mostly supply-side- inflationary pressure without triggering a financial crisis.

The paper is as follows. Sections 2 and 3 introduce the new core inflation measure and its estimation strategy. Sections 4 and 5 discuss the estimation results and provide insights into the structural determinants of core and cyclical inflation. Section 6 discusses some policy implications, while Section 7 assesses the properties of our new core inflation measure. Finally, in Section 8, we conclude. The Online Appendix reports additional details concerning the literature review, the dataset, and the empirical results.

2. The *structural* core inflation rate

Consider the following decomposition of headline inflation into a medium to long-term or trend (core) component π_t^c, a short-term or cyclical (non-core) component π_t^{nc}, and a residual, non-systematic or

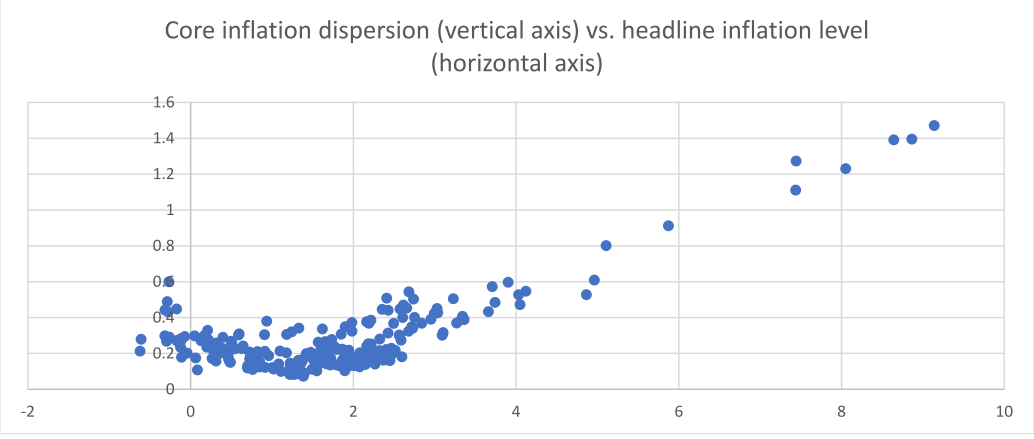

Fig. 1. Cross plot of core inflation dispersion vs. headline inflation level. The cross-sectional standard deviation of the spreads of the various ECB internal core inflation series relative to the Ex-Food and Energy core inflation rate measures core inflation dispersion at each point in time. Each dot refers to a monthly observation over the 1999:1–2022:8 sample period. The ECB internal core inflation series are the Supercore, the Persistent and Common Component of Inflation, the Persistent and Common Component of Inflation computed using the Ex-Food and Energy inflation rate, the Trimmed Mean inflation rate with 10% and 30% symmetric trimming, and the Weighted Median inflation rate.

shock component π_t^r, i.e.,

$$\pi_t = \pi_t^c + \pi_t^{nc} + \pi_t^r. \tag{1}$$

The above decomposition is consistent with Eckstein (1981), where core inflation is defined as "the rate that would occur on the economy's long-term growth path, provided the path were free of shocks ($\pi_t^r = 0$), and the state of demand were neutral in the sense that markets were in long-run equilibrium ($\pi_t^{nc} = 0$)". Under the above conditions, $\pi_t = \pi_t^c$, i.e., core inflation measures the steady-state rate of inflation. In Eckstein's theory core inflation reflects "those price increases made necessary by the increases in the trend costs of the inputs to production." (Eckstein, p. 8), which, in turn, depend on the long-term inflation expectations embodied in nominal interest rates and equity yields and underlying wage claims. Hence, $\pi_t^c = g(\pi_t^e)$, where $g(\cdot)$is a real-valued, monotonic increasing function of the expected inflation rate π_t^e.

The decomposition in (1) can be contrasted with the augmented Phillips curve equation

$$\pi_t = \pi_t^e + slack_{\pi,t} + v_t, \tag{2}$$

where the expected inflation rate π_t^e accounts for inflation persistence, $slack_{\pi,t}$ is the demand-pull, cyclical inflation component, and v_t is the cost-push, supply-side component. In the steady-state we expect

$$\pi_t = \pi_t^e = \pi_t^c = \pi_t^* = \pi_t^m, \tag{3}$$

where π_t^* is the medium to long-term central bank's objective, and therefore tied to monetary inflation dynamics (π_t^m). Hence, in the steady-state equilibrium, expectations are fulfilled, output is at potential, and there are no shocks. It follows that the inflation rate is equal to its expected and core value, equal to the value targeted by the central bank, and equal to the monetary inflation rate, also consistent with Friedman (Friedman, 1969, p. 171)'s quantity theory view, where the general inflation trend is the price change originating from monetary disturbances.

Our measure of core inflation, i.e., the *structural* core inflation rate, allows for deviations of the monetary inflation rate (π_t^m, central banks' generated inflation) from the monetary policy inflation target π_t^*. This is functional to account for the entrenching of persistent supply-side inflation, originating from the structural forces related to globalization -that has been the Great Moderation's chief driver. It is also functional to allow for the entrenching of persistent inflation originating from fiscal policy (π_t^f) along the lines recently formalized by Cochrane (2022). Accordingly, fiscal inflation is generated when public debt exceeds the amount people expect will be repaid in the future, and therefore it will be either defaulted or inflated away. The attempt to get rid of this debt through trading it for other assets or goods and services turns into excess demand and inflation.

Hence, concerning (2), we decompose the supply-side component into two parts, i.e., $v_t = v_{m,t} + v_{s,t}$, reflecting short-term ($v_{s,t}$) and medium to long-term ($v_{m,t}$) supply-side contributions. Moreover, we account for both monetary (π_t^m) and fiscal (π_t^f) sources of demand-side trend inflation ($\pi_t^{mf} = \pi_t^m + \pi_t^f$), and add a residual component ($res_{\pi,t}$), reflecting a non-systematic inflation component subsuming disturbances of various origins, i.e., geopolitical, supply-chains, energy inputs, weather-related, etc., affecting relative price changes, yielding

$$\begin{aligned} \pi_t &= \pi_t^m + \pi_t^f + slack_{\pi,t} + v_{m,t} + v_{s,t} + res_{\pi,t}, \\ &= \left(\pi_t^{mf} + v_{m,t}\right) + \left(slack_{\pi,t} + v_{s,t}\right) + res_{\pi,t}, \\ &= \pi_t^c + \pi_t^{nc} + res_{\pi,t} \end{aligned} \tag{4}$$

where

$$\pi_t^c = E\left[\pi_t \middle| I_{MLT,t}\right] = \pi_t^{mf} + v_{m,t}, \tag{5}$$

and $I_{MLT,t}$ is the information set reflecting medium to long-term macro-financial conditions, which are expected to be informative about the structural drivers of the inflation trend, i.e., the monetary, fiscal, and supply-side components;

$$\pi_t^{nc} = E\left[\pi_t \middle| I_{ST,t}\right] = slack_{\pi,t} + v_{s,t}, \tag{6}$$

and $I_{ST,t}$ is the information set reflecting short-term macro-financial conditions, which are expected to be informative about the structural drivers of cyclical inflation, i.e., its demand and supply-side components;

$$res_{\pi,t} = \pi_t - E\left[\pi_t \middle| I_{MLT,t}\right] - E\left[\pi_t \middle| I_{ST,t}\right], \tag{7}$$

that is, the residual, unexpected, or shock inflation component.

Hence, structural forces are accounted for, such as the disinflationary contribution of the globalization of products (supply chains), labor, financial markets, and potential fiscal inflation. Monetary inflation is also accounted for, modulating the entrenching of persistent fiscal and supply-side developments in the core rate. Cyclical inflation also accounts for demand-pull and supply-side drivers. Its demand-pull component reflects the contribution of short-term aggregate demand pressures. Its supply-side part reflects short-term firms' production decisions triggered by cyclical profitability fluctuations, as determined, among other factors, by systematic developments in energy, transport, and labor costs affecting firms' marginal costs. Non-systematic inflationary pressure stemming from geopolitical, climatic, or other factors market disruption is finally accounted for by the residual component. Within our context, the pass-through from cyclical to core inflation might be further allowed through the non-orthogonality of the core and non-core parts. Yet even under their orthogonality, persistent fiscal and supply-side changes are already entrenched in the core rate, as they are explicitly included in the measure of core inflation. Jarocinski and Lenza (2018), Bobeica and Jarocinski (2019), and Ball and Mazumder (2021) show that an adequately specified Phillips curve can account for inflation or core inflation developments in the euro area, providing support to our modeling of inflationary pressure. Yet, as shown below, our econometric modeling of the inflation trend differs from previous literature contributions. Following Morana, 2021, we estimate the core inflation measure within a model of twenty-eight macroeconomic and financial variables. This is a major improvement relative to small-scale structural common trend models (Bagliano et al., 2002; Hasenzagl et al., 2022). This data-rich modeling framework grants information content and decomposition accuracy, allowing for a dissection of headline and core inflation into parts with clear-cut economic interpretation. Moreover, our trend inflation definition is not grounded on the statistical knowledge of its DGP but, similar in spirit to Hodrick and Prescott (1997), on stylized facts concerning the sources of macroeconomic and financial fluctuations. This grants robustness to trend specification to our core inflation measure. Supportive Monte Carlo results are reported in Morana (2021).

3. Econometric methodology

Following Morana (2021), consider the vector of N weakly stationary or trend stationary macroeconomic and financial variables of interest $\{\mathbf{y}_t\}$, characterized by common medium to long-term and short-term fluctuations. A multivariate *MLT-ST* decomposition can then be written as

$$\mathbf{y}_t = \mathbf{n}_t + \mathbf{a}_t, \tag{8}$$

where $\mathbf{n}_t$ is the $(N \times 1)$ vector of medium to long-term (*MLT*) components, and $\mathbf{a}_t$ is the $(N \times 1)$ zero-mean vector of the short-term (*ST*) components. The vectors $\mathbf{n}_t$ and $\mathbf{a}_t$ are assumed to be orthogonal. The decomposition is implemented by means of a two-step procedure, based on sequential univariate *MLT-ST* decompositions and principal components analysis.

3.1. First step: univariate MLT-ST decomposition

Consider the generic q element in the vector $\mathbf{y}_t$, i.e., $y_{q,t}, q = 1,..,N$. The generic univariate decomposition is then

$$y_{q,t} = n_{q,t} + a_{q,t}, \tag{9}$$

where $\{n_{q,t}\} \equiv \{g(\mathbf{v}_t^*)\}$and $\{a_{q,t}\}$are the generic *MLT* and *ST* components, respectively. It is assumed that $\{a_{q,t}\}$is zero mean and orthogonal to $\{n_{q,t}\}$. Moreover, the real valued function $g(\cdot)$ is

$$g(\mathbf{v}_t^*) = \theta_0 + \theta_1 t + f(\mathbf{x}_t^*), \tag{10}$$

where $f(\mathbf{x}_t^*)$ is the trigonometric polynomial

$$\begin{aligned} f(\mathbf{x}_t^*) = & \sum_{j=1}^{j^*} \theta_{s,j} \sin\left(2\pi j \frac{t}{T}\right) + \theta_{c,j} \cos\left(2\pi j \frac{t}{T}\right) + \\ & \sum_{i=1}^{m} \sum_{j=1}^{j^*} \theta_{s,ij} \sin\left(2\pi j \frac{\sum_{k=1}^{t} x_{i,k}}{\sum_{k=1}^{T} x_{i,k}}\right) + \theta_{c,ij} \cos\left(2\pi j \frac{\sum_{k=1}^{t} x_{i,k}}{\sum_{k=1}^{T} x_{i,k}}\right), \end{aligned} \tag{11}$$

$\mathbf{v}_t^* = [1 \quad t \quad x_{1,t} \quad \cdots \quad x_{m,t}]'$ is a $(m+2) \times 1$ vector; the conditioning variables $x_{i,t}, i = 1,..,m$, are weakly stationary variables with $\sum_{k=1}^{T} x_{i,k} \neq 0$; $\theta_0, \theta_1, \theta_{s,j}, \theta_{c,j}, \theta_{s,ij}, \theta_{c,ij}$ are parameters. The *MLT* component then bears the interpretation of conditional expectation for the series $y_{q,t}$, i.e., $n_{q,t} = E\left[y_{q,t} \middle| \mathbf{v}_t^*\right]$.

Hence, in our context, we assume that the medium to long-term component or trend function DGP is unknown. Based on (a special case of) the Weierstrass Approximation Theorem, we then approximate this unknown function using a trigonometric polynomial specification, whose order j^* is set according to stylized facts concerning economic fluctuations, similar in spirit to Hodrick and Prescott (1997). Empirically, financial cycles in developed countries show a typical periodicity of fifteen to twenty years, lasting much longer than business cycle episodes, whose historical duration has not exceeded eight or ten years in most countries (Borio, 2014; Borio, Drehmann, & Xia, 2019; Beaudry, Galizia, & Portier, 2020). Hence, the index j^* is set to a value such that the *MLT* component shows fluctuations with periodicity P^* consistent with the financial cycle and therefore longer than business cycle episodes, i.e., $j^* = P^*/T$. On the other hand, business cycle fluctuations are accounted by the *ST* component, as $a_{q,t} = y_{q,t} - n_{q,t}$, and $E\left[a_{q,t} \middle| \mathbf{v}_t^*\right] = 0$.

3.1.1. Empirical implementation

Empirically, the decomposition for the generic q element in the vector $\mathbf{y}_t$ is implemented through OLS estimation of the regression model

$$\begin{aligned} y_{q,t} = & \theta_0 + \theta_1 t + \sum_{j=1}^{j^*} \theta_{s,j} \sin\left(2\pi j \frac{t}{T}\right) + \theta_{c,j} \cos\left(2\pi j \frac{t}{T}\right) + \\ & \sum_{i=1}^{m} \sum_{j=1}^{j^*} \theta_{s,ij} \sin\left(2\pi j \frac{\sum_{k=1}^{t} x_{i,k}}{\sum_{k=1}^{T} x_{i,k}}\right) + \theta_{c,ij} \cos\left(2\pi j \frac{\sum_{k=1}^{t} x_{i,k}}{\sum_{k=1}^{T} x_{i,k}}\right) + \varepsilon_{q,t}, \end{aligned} \tag{12}$$

where $t = 1, .., T$, $\varepsilon_{q,t}$ is i.i.d. with zero mean, variance σ^2, and finite fourth moment, and the regressors $x_{i,t}, i = 1,\ldots,m$, are weakly stationary processes. Under the above conditions, OLS estimation of the model in (12) is consistent and asymptotically normal (Morana, 2021; Hamilton, 1994; ch. 16).

Model selection can be implemented within a general to specific reduction approach, using Newey-West standard errors in case of nonspherical residuals, even through an autometrics procedure (Castle, Doornik, & Hendry, 2021), as, for instance, available in the OxMetrics 9 package. We then have

$$y_{q,t} = \hat{n}_{q,t} + \hat{a}_{q,t}, \tag{13}$$

where $\hat{n}_{q,t} \equiv \hat{y}_{q,t}$, i.e., the fitted component from the OLS regression in (12), and $\hat{a}_{q,t} \equiv \hat{\varepsilon}_{q,t}$, i.e., the estimated residual component. The algebra of OLS ensures that the two estimated components are orthogonal by construction. Proceeding sequentially, i.e., series by series, we obtain the multivariate decomposition

$$\mathbf{y}_t = \hat{\mathbf{n}}_t + \hat{\mathbf{a}}_t, \tag{14}$$

where the $(N \times 1)$ vectors $\hat{\mathbf{n}}_t$ and $\hat{\mathbf{a}}_t$ contain the estimated *MLT* and *ST* components, respectively.

3.2. Second step: common MLT and ST components estimation

In the second step, the common medium to long-term and short-term components are computed using Principal Components Analysis (PCA) implemented on each set of estimated univariate components. At this stage, we assume that the $\hat{\mathbf{n}}_t$ components are also zero-mean weakly-stationary or suitably transformed to be made zero-mean weakly stationary.

We have

$$\hat{\mathbf{f}}_{\mathbf{n},t} = \hat{\mathbf{D}}_{\mathbf{n}}^{-1/2} \hat{\mathbf{Q}}_{\mathbf{n}}' \hat{\mathbf{n}}_t, \tag{15}$$

the $s \times 1$ vector of the common *MLT* factors, as estimated by the s standardized principal components for the *MLT* series, where $\hat{\mathbf{D}}_{\mathbf{n}} = diag\{\hat{\lambda}_{\mathbf{n}_1}, \hat{\lambda}_{\mathbf{n}_2}, \ldots, \hat{\lambda}_{\mathbf{n}_s}\}$ is the $s \times s$ diagonal matrix of the non-zero ordered eigenvalues of the sample variance–covariance matrix of the *MLT* processes $\hat{\Sigma}_{\mathbf{n}}$ (rank $s < N$), $\hat{\mathbf{Q}}_{\mathbf{n}}$ is $N \times s$ matrix of the associated orthogonal eigenvectors. Moreover,

$$\hat{\mathbf{f}}_{\mathbf{a},t} = \hat{\mathbf{D}}_{\mathbf{a}}^{-1/2} \hat{\mathbf{Q}}_{\mathbf{a}}' \hat{\mathbf{a}}_t, \tag{16}$$

the $r \times 1$ vector of the common *ST* factors, as estimated by the r standardized principal components of the *ST* series, where $\hat{\mathbf{D}}_{\mathbf{a}} = diag\{\hat{\lambda}_{\mathbf{a}_1}, \hat{\lambda}_{\mathbf{a}_2}, \ldots, \hat{\lambda}_{\mathbf{a}_r}\}$ is the $r \times r$ diagonal matrix of the non-zero ordered eigenvalues of the sample variance–covariance matrix of the *ST* processes $\hat{\mathbf{\Sigma}}_{\mathbf{a}}$ (rank $r < N$), $\hat{\mathbf{Q}}_{\mathbf{a}}$is $N \times r$ matrix of the associated orthogonal eigenvectors. A conjecture of $min\{\sqrt{N}, \sqrt{T}\}$consistency and asymptotic normality of the PC estimator of the common factors $\hat{\mathbf{f}} = [\hat{\mathbf{f}}_{\mathbf{n}}' \quad \hat{\mathbf{f}}_{\mathbf{a}}']'$for the space spanned by the latent factors, based on Bai (2003) and the consistent estimation of the *MLT* and *ST* components, is discussed in Appendix 1.

3.2.1. An economic interpretation of the common factors

Once the common *MLT* ($\hat{\mathbf{f}}_{\mathbf{n},t}$) and *ST* ($\hat{\mathbf{f}}_{\mathbf{a},t}$) factors are estimated, the PC-regression model can be set up

$$\mathbf{y}_t - \hat{\boldsymbol{\mu}}_t = \Theta_{\mathbf{n}}' \hat{\mathbf{f}}_{\mathbf{n},t} + \Theta_{\mathbf{a}}' \hat{\mathbf{f}}_{\mathbf{a},t} + \boldsymbol{\varepsilon}_t, \tag{17}$$

where $\hat{\boldsymbol{\mu}}_t$ is the $N \times 1$ vector of estimated deterministic components, or simply the $N \times 1$ sample mean vector for $\mathbf{y}_t$ under weak stationarity ($\hat{\boldsymbol{\mu}}_t \equiv \hat{\boldsymbol{\mu}}$), $\Theta_{\mathbf{n}}'$ and $\Theta_{\mathbf{a}}'$ are $N \times s$ and $N \times r$ common factor loading matrices, ε_t is i.i.d. with zero mean vector and Σ variance–covariance matrix. The PC-regression in (17) can then be estimated by

$$\mathbf{y}_t - \hat{\boldsymbol{\mu}}_t = \hat{\boldsymbol{\Theta}}_{\mathbf{n}}' \hat{\mathbf{f}}_{\mathbf{n},t} + \hat{\boldsymbol{\Theta}}_{\mathbf{a}}' \hat{\mathbf{f}}_{\mathbf{a},t} + \hat{\boldsymbol{\varepsilon}}_t, \tag{18}$$

where $\hat{\boldsymbol{\Theta}}_{\mathbf{n}}'$is the estimated $N \times s$ common *MLT* factor loading matrix, $\hat{\Theta}_{\mathbf{a}}'$is the estimated $N \times r$ common *ST* factor loading matrix,

$\widehat{\boldsymbol{\varepsilon}}_t = \mathbf{y}_t - \widehat{\boldsymbol{\mu}}_t - \widehat{\boldsymbol{\Theta}}_{\mathbf{n}}^{'}\widehat{\mathbf{f}}_{\mathbf{n},t} - \widehat{\boldsymbol{\Theta}}_{\mathbf{a}}^{'}\widehat{\mathbf{f}}_{\mathbf{a},t}$ is a $N\times 1$ vector of overall idiosyncratic components. Estimation of the common factor loading matrices is performed by OLS, i.e., through the orthogonal projection of (the detrended or demeaned) $\mathbf{y}$ on $\widehat{\mathbf{f}}_{\mathbf{n}}$ and $\widehat{\mathbf{f}}_{\mathbf{a}}$. Hence, consider the $(s+r)\times 1$ vector $\mathbf{f}_t$

$$\widehat{\mathbf{f}}_t = \begin{bmatrix} \widehat{\mathbf{f}}_{\mathbf{n},t} \\ \widehat{\mathbf{f}}_{\mathbf{a},t} \end{bmatrix},$$

the $N\times(r+s)$ factor loading matrices estimator $\widehat{\boldsymbol{\Theta}}^{'} = [\,\widehat{\boldsymbol{\Theta}}_{\mathbf{n}}^{'} \quad \widehat{\boldsymbol{\Theta}}_{\mathbf{a}}^{'}\,]$ is

$$\widehat{\boldsymbol{\Theta}}^{'} = \left[\sum_{t=1}^{T}\mathbf{y}_t\widehat{\mathbf{f}}_t^{'}\right]\left[\sum_{t=1}^{T}\widehat{\mathbf{f}}_t\widehat{\mathbf{f}}_t^{'}\right]^{-1} \tag{19}$$

and

$$\widehat{\boldsymbol{\Sigma}} = \frac{1}{T}\sum_{t=1}^{T}\widehat{\boldsymbol{\varepsilon}}_t\widehat{\boldsymbol{\varepsilon}}_t^{'}. \tag{20}$$

Under the general conditions in Bai (2003) and Bai and Ng (2006), it can be conjectured that the OLS estimator in (19) is $\sqrt{T}$ consistent and asymptotically normal (see Appendix 1). In the case of non-spherical residuals, inference on the estimated loadings can be made using Newey-West HACSE. An economic interpretation of the principal components extracted from the set of estimated *MLT* and *ST* components can be provided by means of their factor loadings $\widehat{\boldsymbol{\Theta}}$ and the proportion of variance of the actual series they account for. See Appendix 2 for further details.

3.3. Measuring core, cyclical, and residual inflation

Following the above-detailed procedure, headline inflation (π_t) is decomposed into three orthogonal components, i.e., core or medium to long-term inflation (π_t^c), cyclical or short-term inflation (π_t^{nc}), and residual inflation ($res_{\pi,t}$). The decomposition can be performed through OLS estimation of the PC-regression

$$\pi_t = \mu_\pi + \sum_{i=1}^{s}\beta_i\widehat{f}_{\mathbf{n}_i,t} + \sum_{i=s+1}^{s+r}\beta_i\widehat{f}_{\mathbf{a}_i,t} + \varepsilon_t, \tag{21}$$

where ε_t is i.i.d. with zero mean, variance σ^2, and finite fourth moment.

Then, the core inflation component is

$$\pi_t^c \equiv E\left[\pi_t\middle|\widehat{\mathbf{f}}_{\mathbf{n},t}\right] = \widehat{\mu}_\pi + \sum_{i=1}^{s}\widehat{\beta}_i\widehat{f}_{\mathbf{n}_i,t}, \tag{22}$$

and bears the interpretation of *conditional expectation* for headline inflation, where the information set includes the components in the $\widehat{\mathbf{f}}_{\mathbf{n},t}$ vector informative on medium to long-term demand-side (monetary and fiscal) and supply-side inflation. The modeling of the expectation component in (22) is much richer than in the standard NKPC, where $E_t\pi_{t+1}$ is replaced by π_t or π_{t-1}, yielding a reduced form model where inflation persistence is accounted by lagged inflation, rather than by medium to long-term structural components.

The cyclical inflation component is

$$\pi_t^{nc} \equiv E\left[(\pi_t - \widehat{\mu}_\pi)\middle|\widehat{\mathbf{f}}_{\mathbf{a},t}\right] = \sum_{i=s+1}^{s+r}\widehat{\beta}_i\widehat{f}_{\mathbf{a}_i,t}, \tag{23}$$

and bears the interpretation of *conditional expectation* for (demeaned) headline inflation, where the information set includes the components in the $\widehat{\mathbf{f}}_{\mathbf{a},t}$ vector informative on short-term demand-side and supply-side inflation.

The residual inflation component is

$$\begin{aligned} res_{\pi,t} &\equiv \pi_t - E\left[\pi_t\middle|\widehat{\mathbf{f}}_{\mathbf{n},t},\widehat{\mathbf{f}}_{\mathbf{a},t}\right] \\ &\equiv \pi_t - \left(\widehat{\mu}_\pi + \sum_{i=1}^{s}\widehat{\beta}_i\widehat{f}_{\mathbf{n}_i,t} + \sum_{i=s+1}^{s+r}\widehat{\beta}_i\widehat{f}_{\mathbf{a}_i,t}\right) \end{aligned} \tag{24}$$

and bears the interpretation of unexpected inflation, yielding a measure of non-sistematic/idiosyncratic inflation developments.

3.3.1. A comparison with the new Keynesian Phillips curve

Comparison of our inflation Eq. (21) with the hybrid new Keynesian Phillips curve (NKPC)

$$\pi_t = \mu + \alpha E_t\pi_{t+1} + \beta\pi_{t-1} + \gamma slack_t \tag{25}$$

shows that our modeling of the expectation component in (22) is much richer than in the NKPC, where $E_t\pi_{t+1}$ is replaced by $\pi_{t+1} + \omega_t$, i.e., actual next year's inflation and prediction error, yielding the RE specification

$$\pi_t = \mu + \alpha\pi_{t+1} + \beta\pi_{t-1} + \varepsilon_t \tag{26}$$

and $\varepsilon_t = \alpha\omega_t + \gamma slack_t$, or by π_t or π_{t-1}, i.e., current or lagged inflation, yielding, for instance, in the latter case

$$\pi_t = \mu + (\alpha+\beta)\pi_{t-1} + \gamma slack_t + v_t, \tag{27}$$

upon adding the disturbance term v_t. Hence, inflation persistence in the NKPC originates from lagged inflation in all cases. In our context, it originates from the medium to long-term macro-financial factors determining core inflation. Much richer is also the modeling of the slack component in our context, accounted by the short-term macro-financial factors determining business cycle fluctuations rather than the output gap, or the unemployment rate, or, more recently, direct measures of labor market tightness.

4. Empirical results

The dataset consists of twenty-eight monthly time series for the euro area over 1999:1–2022:8. The data extensively covers real, nominal, and financial conditions. See Table 1 for the list of variables and the Online Appendix for details about data definitions and construction. In light of the scope of the analysis, the polynomial specifications used for the first-step sequential univariate decompositions only include the linear time trend (t) and the €-coin GDP growth rate ($x_{1,t} \equiv €g_t$; $m = 1$). Moreover, given the sample size available, the maximum order of the trigonometric expansion is $j^* = 2$, to yield *MLT* components associated with GDP growth fluctuations with periodicity larger than ten years. Hence, the econometric specification in (12) is

$$\begin{aligned} y_{q,t} = \; & \theta_0 + \theta_1 t + \sum_{j=1}^{2}\theta_{s,j}\sin\left(2\pi j\frac{t}{T}\right) + \theta_{c,j}\cos\left(2\pi j\frac{t}{T}\right) + \\ & \sum_{j=1}^{2}\theta_{s,1j}\sin\left(2\pi j\frac{\sum_{k=1}^{t}x_{1,k}}{\sum_{k=1}^{T}x_{1,k}}\right) + \theta_{c,1j}\cos\left(2\pi j\frac{\sum_{k=1}^{t}x_{1,k}}{\sum_{k=1}^{T}x_{1,k}}\right) + \varepsilon_{q,t}, \end{aligned} \tag{28}$$

for any series but the €-coin GDP growth rate, for which $\theta_{s,1j} = \theta_{c,1j} = 0$ for any j, to avoid the inclusion of its contemporaneous trigonometric transforms in the set of conditioning regressors. The final econometric models obtained through a general to specific reduction strategy and OLS estimation are reported in Table A1, Panels A-C in the Online Appendix. In the same Table, we also report the KPSS stationarity tests for the actual variables and estimated residuals. The final econometric models are rather parsimonious, but in all cases, apart from the credit gap, various €-coin GDP growth rate transforms are retained, consistent with the association of the estimated *MLT* components with low-

Table 1
Dataset composition.

Data	Source	Data	Source
€-coin GDP growth	BoI	Total credit to the private nonfinancial sectors-to-GDP ratio	BIS
Harmonized unemployment rate	Eurostat	House price index-to-GDP ratio	OECD
Current account-to-GDP ratio	OCED	House price index-to-net disposable income per head ratio	OECD
Fiscal deficit-to-GDP ratio	ECB	House price index-to-rent ratio	OECD
Harmonized CPI	Eurostat	Real gold price index return	IMF
Real earnings for manufacturing growth rate	OECD	Real European Fama-French market factor return	F-F
Real narrow effective exchange rate return	BIS	3-month Euribor rate - €STR spread	ECB
Global supply-chain pressure index	NY Fed	10-year government bond rate - €STR spread	ECB
Real energy price index return	IMF	Composite Indicator of Systemic Sovereign Stress SovCISS	ECB
Real Euro Short-Term Rate €STR	ECB	Euro Soxx 50 (implied) Volatility VSTOXX	Eurex
Real 3-month Euribor rate	ECB	New Composite Indicator of Systemic Stress New-CISS	ECB
Real 10-year government bond rate	ECB	Real European Fama-French size factor return	F-F
Real M3 index of notional stocks growth rate	ECB	Real European Fama-French value factor return	F-F
Excess nominal M3 growth	ECB/BoI	Real European Charart momentum factor return	F-F

frequency GDP fluctuations, i.e., with periodicity larger than ten years. The residual estimated *ST* components are then associated with relatively higher frequency fluctuations, with a periodicity of up to ten years. The decomposition is successful in all cases, as weak stationarity is always detected in the short-term components. The *MLT-ST* decomposition for the various series is reported in Figs. A1-A7 in the Online Appendix.

The estimated *MLT* and *ST* components are then employed in the second-step Principal Components Analysis (PCA). Concerning the inflation rate, excess nominal money growth rate, and real short and long-term interest rates *MLT* components, their changes, rather than levels, are employed in the analysis. The latter transformation raises their average (absolute) pairwise correlation and should make extracting their monetary policy common component more accurate.[1] This transformation is also economically meaningful as it delivers the monthly variation in the series of interest. PCA results are reported in Table 2. In particular, in Panels A and B, we report the sample eigenvalues and the proportion of total variance accounted for by each principal component for the *MLT* and *ST* components, respectively; moreover, in Table A2 in the Online Appendix we report the associated sample eigenvectors ($\widehat{\mathbf{D}}_{\mathbf{n}}^{-1/2}\widehat{\mathbf{Q}}_{\mathbf{n}}^{'}$ and $\widehat{\mathbf{D}}_{\mathbf{a}}^{-1/2}\widehat{\mathbf{Q}}_{\mathbf{a}}^{'}$). As shown in Table 2, in light of the proportion of total variance accounted for by each principal component, we report results for the first four PCs only, which cumulatively accounts for over 60% of the total variance for both sets of series (70% for the *MLT* series; 63% for the *ST* series). The first principal component ($PC_{\mathbf{n}_1,t} = \widehat{\mathbf{Q}}_{\mathbf{n}_1}^{'}\widehat{\mathbf{n}}_t$; $PC_{\mathbf{a}_1,t} = \widehat{\mathbf{Q}}_{\mathbf{a}_1}^{'}\widehat{\mathbf{a}}_t$) alone accounts for about 30% of total variance; the second and third components account for additional 17% and 12% of variance for both sets of series. The fourth component accounts for 11% (7%) of *MLT* (*ST*) total variance. In light of the small proportion of accounted total variance, we neglect the remaining higher-order principal components. Finally, in Table 2, Panels A-B, we also report the estimated signal-to-noise ratio from local trend model U.C. models for the selected common *MLT* and *ST* components to assess the empirical relevance of PC's measurement error (see Appendix 1).[2] As the estimated inverse signal-to-noise ratio is zero or virtually zero for all the estimated PCs, we can then neglect it and expect standard asymptotic theory to allow for valid inference in the PC-regression analysis.

4.1. PCs economic interpretation and information content

We base the economic interpretation of the selected common factors on the results of the PC regressions, which yield information on the mean impact ($\widehat{\boldsymbol{\Theta}}$ in (19); Table 3) and the proportion of accounted variance (Table 4) for each variable by any common factor ($\widehat{\mathbf{f}}_{\mathbf{n}_i}, \widehat{\mathbf{f}}_{\mathbf{a}_i}$). The estimated coefficients in $\widehat{\boldsymbol{\Theta}}$ should be interpreted in terms of loadings, providing information about how each variable behaves along the scenario described by each common factor. Similar information follows from the PCs' composition, i.e., the sample eigenvectors (Table A2, Online Appendix). The general interpretation we provide to the principal components is of stylized facts describing macro-financial interactions in the eurozone. Stylized facts are empirical regularities that have persistently shaped the macroeconomic and financial environment since the inception of the euro area and concern the joint evolution of subsets of variables. The financial and business cycles are exemplifications of the features. Still, others can be envisaged in light of the prevailing macroeconomic regime in the sample, i.e., the Great Moderation. The Great Moderation resulted from improved economic policy management and favorable supply-side shocks (globalization), increasing potential growth and reducing production costs. Apart from globalization forces, economic policy, particularly monetary policy, was challenged to maintain macro-financial stability in the face of a sequence of episodes of financial instability that have dragged on from the late 1990s, hitting housing, commodity, stock, and sovereign bond markets and culminating with the Great Recession and the sovereign debt crisis in the euro area (Bagliano & Morana, 2017). We find that $\widehat{\mathbf{f}}_{\mathbf{n}_1}$ convey information on macro-financial interactions associated with the financial cycle, and $\widehat{\mathbf{f}}_{\mathbf{a}_1}$ and $\widehat{\mathbf{f}}_{\mathbf{a}_2}$ with the business cycle, about its demand and supply-side determinants. $\widehat{\mathbf{f}}_{\mathbf{n}_2}$ convey information on medium to long-term supply-side developments, and $\widehat{\mathbf{f}}_{\mathbf{n}_3}$ and $\widehat{\mathbf{f}}_{\mathbf{n}_4}$ on medium to long-term fiscal and monetary policy management, respectively. Finally, $\widehat{\mathbf{f}}_{\mathbf{a}_3}$, $\widehat{\mathbf{f}}_{\mathbf{a}_4}$ yield information on short-term financial developments. In the Online Appendix, we report a comprehensive account of the economic interpretation of the selected PCs (see also Figs. A8 and A9).

In light of the scope of the paper, below we focus on those stylized facts most informative to account for inflation variability historically, i.e., $\widehat{\mathbf{f}}_{\mathbf{n}_2}, \widehat{\mathbf{f}}_{\mathbf{n}_3}, \widehat{\mathbf{f}}_{\mathbf{n}_4}, \widehat{\mathbf{f}}_{\mathbf{a}_1}$, and $\widehat{\mathbf{f}}_{\mathbf{a}_2}$. Without loss of generality, in what follows, we consider $-\widehat{\mathbf{f}}_{\mathbf{n}_2}$,$-\widehat{\mathbf{f}}_{\mathbf{n}_3}$, and $-\widehat{\mathbf{f}}_{\mathbf{a}_2}$ to ease their economic interpretation. The transformation is immaterial concerning the estimation of the common components, implying the sign inversion of the associated loadings[3]. We plot the selected principal components in Fig. 2. The plots also include details about the timing of recessions and financial distress episodes since the early 2000s. In the plots, light grey shaded areas refer to

[1] The impact is particularly sizable on the correlations between the inflation rate and the overnight (+0.27) and long-term (+0.55) real interest rates (not reported).

[2] Only for $PC_{\mathbf{n}_4,t}$, we also include an unobserved AR-2 component. Detailed results are available upon request.

[3] Note that $\theta f = \theta^* f^* = \theta(-1)(-1)f$.

Table 2
Principal components analysis.

Panel A: Selected estimated eigenvalues, medium to long-term components

	PC_1	PC_2	PC_3	PC_4	PC_5	PC_6	PC_7	PC_8
EigenVa	8.75	4.66	3.39	2.93	2.05	1.83	1.37	1.26
% *var*	31.26	16.63	12.09	10.46	7.33	6.55	4.88	4.50
% *cum*	31.26	47.89	59.99	70.44	77.77	84.32	89.20	93.70
$(\mathbf{s}/\mathbf{n})^{-1}$	0.0024	0.0000	0.0286	0.0488	–	–	–	–

Panel B: Selected estimated eigenvalues, short-term components

	PC_1	PC_2	PC_3	PC_4	PC_5	PC_6	PC_7	PC_8
EigenVa	7.16	5.16	3.36	2.00	1.60	1.16	1.09	0.97
% *var*	25.57	18.43	11.98	7.13	5.70	4.16	3.88	3.46
% *cum*	25.57	44.00	55.99	63.12	68.81	72.97	76.85	80.31
$(\mathbf{s}/\mathbf{n})^{-1}$	0.0000	0.0000	0.0000	0.0000	–	–	–	–

Panel A in the Table reports the sample eigenvalues (*EigenVa*) corresponding to the largest eight PCs ($\boldsymbol{PC}_1, \cdots, \boldsymbol{PC}_8$) of the medium to long-term components, their percentage of the accounted total variance (% *var*), the cumulative percentage of the accounted total variance (% *cum*), and the inverse signal-to-noise ratios $(\mathbf{s}/\mathbf{n})^{-1}$. Panel B reports the same statistics for the short-term components.

periods of financial stress and Russia's war in Ukraine; dark grey shaded areas to recessions.

4.1.1. Supply-side medium to long-term disinflationary pressure

$-\widehat{\mathbf{f}}_{\mathbf{n}_2}$ is informative on the medium to long-term disinflationary trend induced in advanced countries by globalization since the 1980s and the concurrent Great Moderation regime. A reversal of these favorable supply-side developments can be read in terms of a persistent increase in $-\widehat{\mathbf{f}}_{\mathbf{n}_2}$. Coherently, $-\widehat{\mathbf{f}}_{\mathbf{n}_2}$ loads the global supply-chain pressure index positively, accounting for 50% of its variance. It also loads positively real energy prices and the inflation rate, and negatively real wages, and accounts for about 15% of their variance (Tables 3 and 4). The negative association with the real wage is consistent with downward nominal wage rigidity. As shown in Fig. 2 (first plot), $-\widehat{\mathbf{f}}_{\mathbf{n}_2}$ has been on a downward/disinflationary trend during all three recessions in the sample. Noticeable is its persistent upward drift in the post-pandemic recession period and its stabilization at levels never experienced since the inception of the euro area. It is too early to establish whether this is the first manifestation of a new macroeconomic regime unfolding ahead, showing high inflation and slow growth (Goodhart & Pradhan, 2020; Spence, 2022) or even a Great Stagflation, as recently argued by Roubini (2022a), Roubini (2022b). However, most favorable supply-side developments during the Great Moderation are at risk of undoing due to demographic factors and de-globalization forces reducing international trade and technological, capital, and migratory flows. The green transition might generate further pressures on energy prices, while persistent environmental degradation might negatively affect agricultural production. Empirically, $-\widehat{\mathbf{f}}_{\mathbf{n}_2}$ in our sample is output-neutral. Yet, as Borio (2022) shows, high and low inflation regimes are very different, notably in their self-reinforcing property through their impact on wage and price settings. In a high-inflation regime, the likelihood of wage-price spirals increases, as the risk of deanchoring agents' expectations and undermining central bank credibility. The 1970s and 1980s stagflation exemplify the above threats (Blinder, 1982).

4.1.2. Economic policy in the medium to long-term

$-\widehat{\mathbf{f}}_{\mathbf{n}_3}$ and $\widehat{\mathbf{f}}_{\mathbf{n}_4}$ are informative on medium to long-term fiscal and monetary policy, respectively. Both policies are countercyclical. An increase in $-\widehat{\mathbf{f}}_{\mathbf{n}_3}$, i.e., a fiscal expansion concurrent with monetary accommodation, contrasts a deterioration in real activity and labor market conditions, improving financial markets and economic sentiments. An increase in $\widehat{\mathbf{f}}_{\mathbf{n}_4}$, i.e., a monetary contraction concurrent with a fiscal contraction, contrasts an inflationary output expansion within a context of abundant liquidity, appreciating housing prices, and destabilizing financial conditions, improving economic sentiments (see Table 3 for supportive evidence). Coherently, as shown in Table 4, $\widehat{\mathbf{f}}_{\mathbf{n}_3}$ is the largest contributor to fiscal deficit to GDP ratio variance (25%). It accounts for 5% of output and inflation variance. $\widehat{\mathbf{f}}_{\mathbf{n}_4}$ is the largest contributor to real interest rates (37%-50%), current account (55%), and credit (29%) variances. It accounts for 2%-3% of output and inflation variance. As shown in Fig. 2 (second and third plot), euro area fiscal and monetary policies were countercyclical in all three recessions in the sample. The fiscal expansion is noticeably shallower during the sovereign debt crisis than the other crises in the sample. A regime change can be noted in ECB monetary policy, separated by the sovereign debt crisis. A relatively tighter monetary stance characterizes the first regime, while the second regime is looser (zero lower bound and Q.E. policy). The transition between the two regimes was smooth; it started during the late phase of the Great Recession and ended during the sovereign debt recession. The monetary policy response was countercyclical on these occasions. The upper spike during the pandemic recession likely signals the increase in the real interest rate determined by the temporary deflation at the zero lower bound. On this occasion, ECB monetary policy was countercyclical by introducing a new round of Q.E., i.e., the Pandemic Emergency Purchase Program (PEPP).

4.1.3. Macro-financial interactions over the business cycle

$\widehat{\mathbf{f}}_{\mathbf{a}_1}$ and $-\widehat{\mathbf{f}}_{\mathbf{a}_2}$ convey information about the business cycle concerning its demand-side and supply-side drivers, respectively. During the building-up phase of the business cycle, output and employment expand, financial assets appreciate, the economic outlook improves, and countercyclical economic policy fosters macro and financial stability. Moreover, a demand-side expansion would pull inflation upward, while a supply-side expansion would push inflation downward. A typical worsening in short-term, cyclical conditions, i.e., the contractionary phase of the business cycle, would be characterized by opposite dynamics to those described above (see Table 3 for supportive evidence). As shown in Table 4, $\widehat{\mathbf{f}}_{\mathbf{a}_1}$ and $\widehat{\mathbf{f}}_{\mathbf{a}_2}$ jointly account for about 40% of output and inflation variances and 76% of stock returns variance. Yet, $\widehat{\mathbf{f}}_{\mathbf{a}_1}$ impacts relatively more on inflation than output and stock returns (35% vs. 14% and 16%), and the other way around for $\widehat{\mathbf{f}}_{\mathbf{a}_2}$ (9% vs. 26% and 60%). $\widehat{\mathbf{f}}_{\mathbf{a}_1}$ and $-\widehat{\mathbf{f}}_{\mathbf{a}_2}$ are plotted in Fig. 2 (fourth and fifth plot). As shown in the plots, demand and supply-side factors contributed to the depth of all three recessions in the sample, i.e., the Great Recession and the recessions associated with the sovereign debt crisis and the pandemic. Noticeable is the negative correlation between the two components since May 2021, pointing to persistent demand-side

Table 3
Regressions of demeaned actual variables on standardized PCs.

	ϵg	u	rw	π	em	ro	rs	rl
$PC_{n,1}$	**0.865**	**−0.035**	−0.004	0.044	**0.827**	**0.160**	−0.002	**−0.521**
	(0.000)	(0.000)	(0.968)	(0.604)	(0.004)	(0.009)	(0.973)	(0.000)
$-PC_{n,2}$	0.089	−0.002	**−0.462**	**0.567**	**0.834**	**−0.731**	**−0.723**	**−0.992**
	(0.503)	(0.469)	(0.000)	(0.000)	(0.000)	(0.000)	(0.000)	(0.000)
$-PC_{n,3}$	**−0.463**	**0.034**	**−0.296**	**0.280**	**0.697**	−0.070	−0.084	0.045
	(0.000)	(0.000)	(0.000)	(0.000)	(0.010)	(0.234)	(0.146)	(0.636)
$PC_{n,4}$	**0.315**	0.001	**0.220**	**0.205**	**0.708**	**1.362**	**1.439**	**1.180**
	(0.007)	(0.657)	(0.006)	(0.025)	(0.053)	(0.000)	(0.000)	(0.000)
$PC_{a,1}$	**0.968**	**−0.025**	**−0.878**	**0.875**	**−1.851**	**−0.736**	**−0.729**	**−0.494**
	(0.000)	(0.000)	(0.000)	(0.000)	(0.000)	(0.000)	(0.000)	(0.000)
$-PC_{a,2}$	**1.094**	**0.009**	0.108	**−0.517**	**−1.139**	**0.475**	**0.418**	**0.532**
	(0.000)	(0.008)	(0.239)	(0.000)	(0.000)	(0.000)	(0.000)	(0.000)
$PC_{a,3}$	−0.168	**0.017**	−0.085	−0.017	0.169	**−0.405**	**−0.351**	−0.018
	(0.228)	(0.000)	(0.247)	(0.839)	(0.620)	(0.000)	(0.000)	(0.880)
$PC_{a,4}$	**−0.326**	**0.013**	−0.022	0.104	0.394	**−0.245**	**−0.251**	−0.016
	(0.002)	(0.000)	(0.768)	(0.226)	(0.091)	(0.000)	(0.000)	(0.828)
$R2$	**0.76**	**0.88**	**0.76**	**0.82**	**0.63**	**0.93**	**0.93**	**0.85**
	sb	hl	mm	rx	ca	lo	fd	hg
$PC_{n,1}$	**0.176**	**0.355**	0.134	**1.416**	**0.485**	**−0.681**	**0.692**	**1.785**
	(0.000)	(0.000)	(0.453)	(0.008)	(0.000)	(0.000)	(0.000)	(0.000)
$-PC_{n,2}$	−0.112	−0.117	−0.101	−0.491	−0.140	**−0.261**	**−0.542**	**0.853**
	(0.062)	(0.057)	(0.251)	(0.259)	(0.152)	(0.000)	(0.000)	(0.000)
$-PC_{n,3}$	**0.112**	**0.549**	0.215	**1.866**	**−0.305**	0.115	**−0.882**	**0.724**
	(0.022)	(0.000)	(0.065)	(0.007)	(0.004)	(0.131)	(0.000)	(0.000)
$PC_{n,4}$	−0.038	**0.353**	0.118	**1.307**	**−1.147**	**−0.182**	**0.427**	−0.104
	(0.348)	(0.000)	(0.370)	(0.045)	(0.000)	(0.040)	(0.000)	(0.335)
$PC_{a,1}$	0.030	**0.441**	−0.203	−0.282	**−0.231**	**0.242**	−0.003	**−0.334**
	(0.288)	(0.000)	(0.113)	(0.628)	(0.001)	(0.000)	(0.974)	(0.014)
$-PC_{a,2}$	**0.331**	−0.002	**−0.315**	**1.369**	**0.321**	0.058	**−0.713**	**0.992**
	(0.000)	(0.973)	(0.027)	(0.002)	(0.001)	(0.434)	(0.000)	(0.000)
$PC_{a,3}$	**0.198**	**−0.698**	**0.365**	**−1.210**	−0.056	**0.387**	**−0.526**	**0.922**
	(0.000)	(0.000)	(0.016)	(0.019)	(0.451)	(0.000)	(0.000)	(0.000)
$PC_{a,4}$	**0.083**	**0.218**	−0.209	**3.170**	0.157	**0.229**	0.115	**−0.269**
	(0.010)	(0.003)	(0.102)	(0.000)	(0.065)	(0.000)	(0.313)	(0.007)
$R2$	**0.70**	**0.71**	**0.28**	**0.56**	**0.81**	**0.77**	**0.80**	**0.87**
	hi	hr	rg	mk	rm	cg	vx	sc
$PC_{n,1}$	**1.779**	**2.641**	**−3.246**	0.156	**1.649**	0.127	**−1.917**	**−0.100**
	(0.000)	(0.000)	(0.008)	(0.077)	(0.000)	(0.519)	(0.011)	(0.000)
$-PC_{n,2}$	**0.611**	**0.959**	**1.866**	**−0.271**	**0.335**	0.239	**2.074**	**0.023**
	(0.000)	(0.000)	(0.043)	(0.001)	(0.047)	(0.363)	(0.000)	(0.000)
$-PC_{n,3}$	**0.420**	0.079	1.701	**0.196**	−0.045	0.325	0.060	0.009
	(0.000)	(0.270)	(0.074)	(0.016)	(0.826)	(0.105)	(0.924)	(0.114)
$PC_{n,4}$	−0.054	**0.369**	1.229	−0.179	**0.817**	**1.399**	**2.248**	−0.007
	(0.628)	(0.000)	(0.168)	(0.065)	(0.005)	(0.000)	(0.000)	(0.285)
$PC_{a,1}$	0.197	**0.965**	−0.237	**0.654**	**−1.759**	**−1.262**	**−3.134**	**0.010**
	(0.219)	(0.000)	(0.796)	(0.000)	(0.000)	(0.000)	(0.000)	(0.049)
$-PC_{a,2}$	0.142	−0.006	**−2.563**	**1.279**	**0.472**	0.412	**−3.639**	**−0.056**
	(0.258)	(0.948)	(0.009)	(0.000)	(0.017)	(0.063)	(0.000)	(0.000)
$PC_{a,3}$	**0.808**	**0.293**	**5.888**	0.037	0.018	**0.445**	**2.648**	**0.026**
	(0.000)	(0.001)	(0.000)	(0.753)	(0.947)	(0.025)	(0.000)	(0.000)
$PC_{a,4}$	**−0.279**	**−0.396**	**−8.821**	−0.041	−0.036	**−0.492**	**1.294**	**0.012**
	(0.005)	(0.000)	(0.000)	(0.638)	(0.836)	(0.019)	(0.019)	(0.006)
$R2$	**0.87**	**0.96**	**0.66**	**0.79**	**0.73**	**0.67**	**0.57**	**0.90**
	so	nc	gs	re				
$PC_{n,1}$	**−0.162**	**−0.102**	0.078	3.116				
	(0.000)	(0.000)	(0.077)	(0.307)				
$-PC_{n,2}$	0.008	**0.046**	**0.594**	**15.33**				
	(0.479)	(0.000)	(0.000)	(0.000)				
$-PC_{n,3}$	−0.014	−0.010	0.043	−2.572				
	(0.318)	(0.300)	(0.265)	(0.555)				
$PC_{n,4}$	**0.077**	**0.032**	**−0.322**	4.792				
	(0.001)	(0.000)	(0.000)	(0.193)				
$PC_{a,1}$	0.007	**−0.031**	**0.167**	**22.87**				
	(0.571)	(0.000)	(0.005)	(0.000)				
$-PC_{a,2}$	**−0.057**	**−0.108**	**−0.086**	4.527				
	(0.001)	(0.000)	(0.014)	(0.126)				
$PC_{a,3}$	**0.054**	**0.041**	**0.141**	6.179				
	(0.014)	(0.000)	(0.004)	(0.071)				
$PC_{a,4}$	−0.006	**0.015**	0.055	−0.104				
	(0.662)	(0.029)	(0.116)	(0.973)				
$R2$	**0.66**	**0.83**	**0.82**	**0.61**				

The Table reports the results of the estimated PC regressions for any of the demeaned monthly variables in the data set on the first four standardized PCs extracted from the MLT ($PC_{n,i}$) and ST ($PC_{a,i}$) series. The figures in bold are statistically significant at the 5% level. Figures in round brackets refer to Newey-West consistent t-ratio p-

values. ***R2*** is the coefficient of determination. The variables are the €-coin GDP growth rate (***€g***), the change in the unemployment rate (***u***), the real wage growth rate (***rw***), the inflation rate (π), the excess money growth rate (***em***), the real overnight, short- and long-term interest rates (***ro, rs, rl***), the Fama-French size, value and market factors (***sb***, ***hl***, ***mk***), the Charart momentum factor (***mm***), the real effective exchange rate return (***rx***), the current account to GDP ratio (***ca***), the fiscal deficit to GDP ratio (***fd***), the term spread (***lo***), the house price to GDP ratio (***hg***), the house price to income ratio (***hi***), and the house price to rent ratio (***hr***), the real gold price return (***rg***), and the real M3 growth rate (***rm***), the credit to GDP ratio (***cg***), the VSTOXX implied volatility index (***vx***), the New-CISS composite financial condition index (***nc***), the Euribor-Eonia spread (***so***), the composite indicator of systemic sovereign stress (***sc***); the monthly NY Fed Global Supply Chain Pressure Index (***gs***), and the real energy price growth rate (***re***).

Table 4
Actual Variables Proportion of Explained Variance by each selected PC.

Var %	*€g*	*u*	*rw*	π	*em*	*ro*	*rs*	*rl*
$PC_{n,1}$	**0.16**	**0.27**	0.00	0.00	**0.06**	**0.01**	0.00	**0.07**
$PC_{n,2}$	0.00	0.00	**0.13**	**0.16**	**0.06**	**0.14**	**0.13**	**0.26**
$PC_{n,3}$	**0.05**	**0.26**	**0.05**	**0.04**	**0.04**	0.00	0.00	0.00
$PC_{n,4}$	**0.02**	0.00	**0.03**	**0.02**	0.04	**0.49**	**0.53**	**0.37**
$PC_{a,1}$	**0.20**	**0.14**	**0.47**	**0.39**	**0.29**	**0.14**	**0.14**	**0.06**
$PC_{a,2}$	**0.25**	**0.02**	0.01	**0.14**	**0.11**	**0.06**	**0.04**	**0.07**
$PC_{a,3}$	0.01	**0.06**	0.00	0.00	0.00	**0.04**	**0.03**	0.00
$PC_{a,4}$	**0.02**	**0.04**	0.00	0.01	0.01	**0.02**	**0.02**	0.00
Var %	*sb*	*hl*	*mm*	*rx*	*ca*	*lo*	*fd*	*hg*
$PC_{n,1}$	**0.10**	**0.08**	0.01	**0.06**	**0.10**	**0.44**	**0.15**	**0.43**
$PC_{n,2}$	**0.04**	0.01	0.01	0.01	0.01	**0.06**	**0.09**	**0.10**
$PC_{n,3}$	**0.04**	**0.19**	0.03	**0.10**	**0.04**	0.01	**0.25**	**0.07**
$PC_{n,4}$	0.00	**0.08**	0.01	**0.05**	**0.55**	**0.03**	**0.06**	0.00
$PC_{a,1}$	0.00	**0.12**	0.03	0.00	**0.02**	**0.06**	0.00	**0.02**
$PC_{a,2}$	**0.37**	0.00	**0.07**	**0.05**	**0.04**	0.00	**0.16**	**0.13**
$PC_{a,3}$	**0.13**	**0.30**	**0.09**	**0.04**	0.00	**0.14**	**0.09**	**0.11**
$PC_{a,4}$	**0.02**	**0.03**	0.03	**0.28**	0.01	**0.05**	0.00	**0.01**
Var %	*hi*	*hr*	*rg*	*mk*	*rm*	*cg*	*vx*	*sc*
$PC_{n,1}$	**0.60**	**0.69**	**0.05**	0.01	**0.30**	0.00	**0.04**	**0.59**
$PC_{n,2}$	**0.07**	**0.09**	**0.02**	**0.03**	**0.01**	0.01	**0.05**	**0.03**
$PC_{n,3}$	**0.03**	0.00	0.01	**0.01**	0.00	0.02	0.00	0.00
$PC_{n,4}$	0.00	**0.01**	0.01	0.01	**0.07**	**0.29**	**0.06**	0.00
$PC_{a,1}$	0.01	**0.09**	0.00	**0.16**	**0.34**	**0.23**	**0.12**	0.01
$PC_{a,2}$	0.00	0.00	**0.03**	**0.60**	**0.02**	0.03	**0.16**	**0.18**
$PC_{a,3}$	**0.12**	**0.01**	**0.17**	0.00	0.00	**0.03**	**0.09**	**0.03**
$PC_{a,4}$	**0.01**	**0.02**	**0.38**	0.00	0.00	**0.04**	**0.02**	**0.01**
Var %	*so*	*nc*	*gs*	*re*				
$PC_{n,1}$	**0.43**	**0.30**	0.01	0.01				
$PC_{n,2}$	0.00	**0.06**	**0.52**	**0.14**				
$PC_{n,3}$	0.00	0.00	0.00	0.00				
$PC_{n,4}$	**0.10**	**0.03**	**0.15**	0.01				
$PC_{a,1}$	0.00	**0.03**	**0.04**	**0.32**				
$PC_{a,2}$	**0.05**	**0.34**	**0.01**	0.01				
$PC_{a,3}$	**0.05**	**0.05**	**0.03**	0.02				
$PC_{a,4}$	0.00	**0.01**	0.01	0.00				

The Table reports the proportion of variance for any of the monthly variables in the data set accounted by the first four standardized PCs extracted from the *MLT* ($PC_{n,i}$) and *ST* ($PC_{a,i}$) series. The figures in bold are statistically significant at the 5% level. The variables are the €-coin GDP growth rate (***€g***), the change in the unemployment rate (***u***), the real wage growth rate (***rw***), the inflation rate (π), the excess money growth rate (***em***), the real overnight, short- and long-term interest rates (***ro, rs, rl***), the Fama-French size, value and market factors (***sb***, ***hl***, ***mk***), the Charart momentum factor (***mm***), the real effective exchange rate return (***rx***), the current account to GDP ratio (***ca***), the fiscal deficit to GDP ratio (***fd***), the term spread (***lo***), the house price to GDP ratio (***hg***), the house price to income ratio (***hi***), and the house price to rent ratio (***hr***), the real gold price return (***rg***), and the real M3 growth rate (***rm***), the credit to GDP ratio (***cg***), the VSTOXX implied volatility index (***vx***), the New-CISS composite financial condition index (***nc***), the Euribor-Eonia spread (***so***), the composite indicator of systemic sovereign stress (***sc***); the monthly NY Fed Global Supply Chain Pressure Index (***gs***), and the real energy price growth rate (***re***).

pressure in the face of deteriorating supply-side conditions.

5. Structural core inflation developments for the euro area

The estimation results for the headline inflation PC regression in (21) are reported in Table 5. To control for the impact of outlying observations and further investigate the source of idiosyncratic inflation, we run a general to specific regression analysis using an autometrics procedure (Castle et al., 2021). This allows for the endogenous selection of impulse dummy variables while considering all the estimated PCs extracted from the *MLT* and *ST* components, unlike the stylized facts assessment stage, where only the selected common components are used. As shown in Table 5 (column 1), three impulse dummies are selected, controlling for the large inflation realizations at the end of the sample, i.e., June, July, and August 2022. Moreover, two idiosyncratic PCs can be retained, i.e., $\widehat{\mathbf{f}}_{\mathbf{n}_7,t}$ and $\widehat{\mathbf{f}}_{\mathbf{n}_9,t}$ (column 2). The augmented regression accounts for about 96% of headline inflation variability. Table 5 reports additional candidate inflation regressions obtained from a second-round reduction analysis. At this stage, we aim to remove from the specification sequentially those PCs not statistically significant ($\widehat{\mathbf{f}}_{\mathbf{n}_1,t}$, $\widehat{\mathbf{f}}_{\mathbf{a}_4,t}$) or accounting only for a minor proportion of inflation variance (1%; $\widehat{\mathbf{f}}_{\mathbf{a}_3,t}$). The accounted variance is virtually unchanged (columns 3 and 4). As a final step, we omit from the inflation equation the impulse dummy variables. As shown in Table 5 (column 5), the coefficient of determination is virtually unchanged, therefore suggesting that the additional idiosyncratic factors $\widehat{\mathbf{f}}_{\mathbf{n}_7,t}$ and $\widehat{\mathbf{f}}_{\mathbf{n}_9,t}$contain sufficient information about the inflationary developments at the end of the sample to make the impulse dummies redundant. In particular, $\widehat{\mathbf{f}}_{\mathbf{n}_9,t}$ accounts for about 10% of inflation variance; it also accounts for 8% of the variance for real energy prices and the supply chain pressure index (not reported), impacting both variables (and inflation) positively. Hence, it is related to idiosyncratic real energy prices and supply-chain developments, likely to carry relevant information on the most recent inflationary pressure. On the other hand, $\widehat{\mathbf{f}}_{\mathbf{n}_7,t}$ is informative about output and inflation during the largest recessions in the sample, i.e., the Great Recession and the pandemic recession. It accounts for about 4% of inflation and 6% of output variance and negatively impacts both variables. Coherently, the omission of the idiosyncratic factors leads to a strong information loss, as the coefficient of determination falls to 0.82 (column 6).

In light of the auxiliary regression results and the information content of the estimated common factors, consistent with the theoretical setting, headline inflation is decomposed into three components: core inflation, non-core or cyclical inflation, and residual inflation. According to their definition in ()()()(22)–(24), we then have

$$\pi_t^c \equiv E\left[\pi_t \middle| \widehat{f}_{\mathbf{n}_2,t}, \widehat{f}_{\mathbf{n}_4,t}, \widehat{f}_{\mathbf{n}_3,t}\right] = \widehat{\mu}_\pi + \widehat{\beta}_1 \widehat{f}_{\mathbf{n}_2,t} + \widehat{\beta}_2 \widehat{f}_{\mathbf{n}_3,t} + \widehat{\beta}_3 \widehat{f}_{\mathbf{n}_4,t}, \tag{29}$$

where core inflation (π_t^c) measures the expected headline inflation rate conditional to the macro-financial information set subsumed by its medium to long-term supply-side ($\widehat{\mathbf{f}}_{\mathbf{n}_2}$) and demand-side ($\widehat{\mathbf{f}}_{\mathbf{n}3}, \widehat{\mathbf{f}}_{\mathbf{n}_4}$) components, respectively. We name the above measure *structural core*

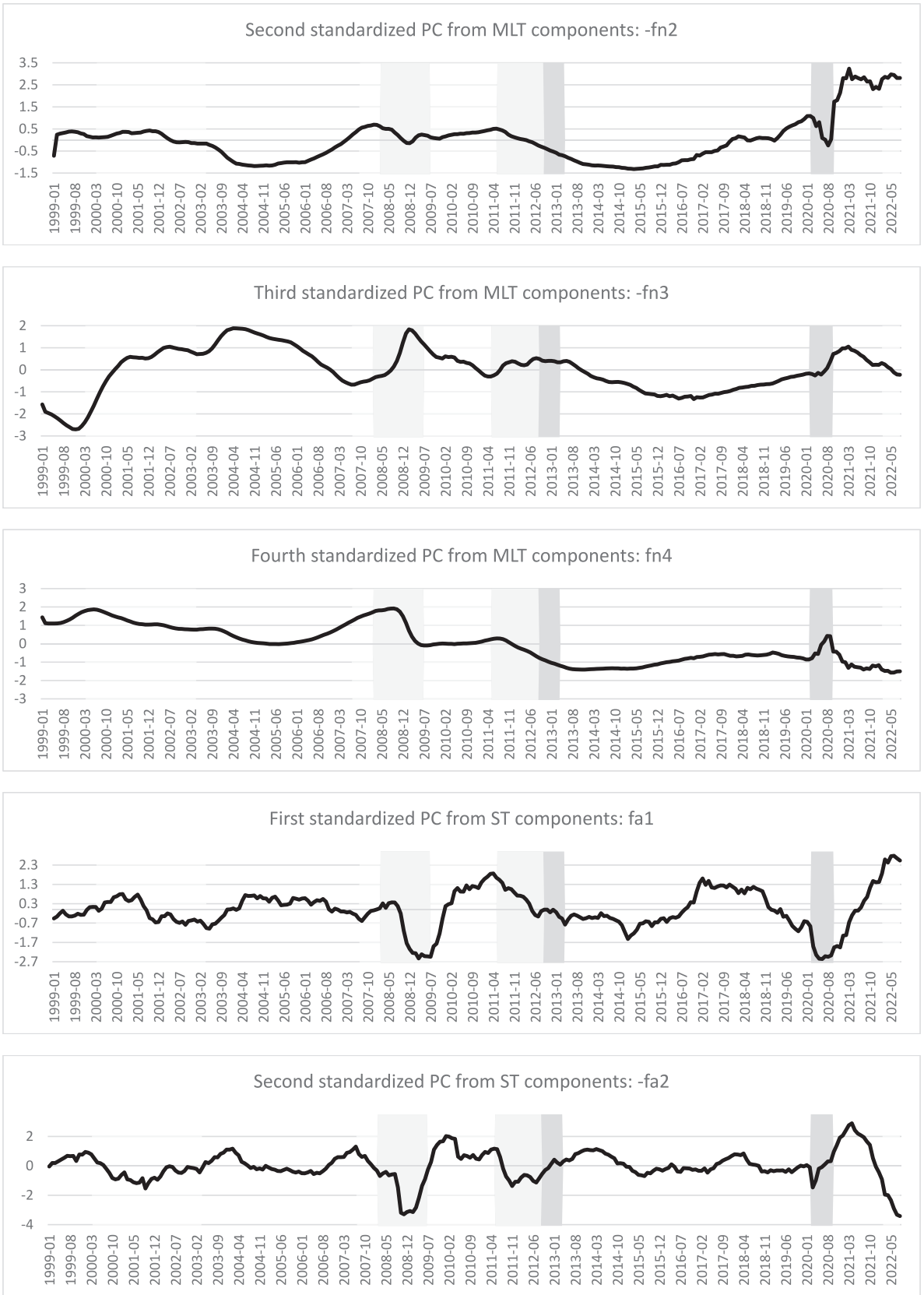

Fig. 2. Standardized principal components from MLT and ST series.

Table 5
Inflation and output regressions on selected standardized PCs.

	π	π	π	π	π	π	$€g$	$€g$	$€g$
$PC_{n,1}$	0.028	0.040	–	–	–	–	0.933	0.873	0.865
	(0.086)	(0.968)					(0.099)	(0.117)	(0.132)
$-PC_{n,2}$	0.500	0.564	0.561	0.563	0.588	0.570	–	–	–
	(0.102)	(0.035)	(0.033)	(0.033)	(0.034)	(0.037)			
$-PC_{n,3}$	0.295	0.299	0.306	0.295	0.291	0.295	−0.507	−0.507	−0.474
	(0.066)	(0.035)	(0.032)	(0.035)	(0.036)	(0.037)	(0.100)	(0.111)	(0.109)
$PC_{n,4}$	0.253	0.234	0.234	0.221	0.204	0.196	0.286	0.272	0.303
	(0.093)	(0.037)	(0.036)	(0.038)	(0.039)	(0.037)	(0.111)	(0.113)	(0.113)
$PC_{a,1}$	0.825	0.731	0.731	0.730	0.740	0.877	0.686	0.815	0.981
	(0.094)	(0.036)	(0.040)	(0.043)	(0.044)	(0.037)	(0.126)	(0.154)	(0.218)
$-PC_{a,2}$	−0.423	−0.346	−0.338	−0.359	−0.390	−0.516	1.012	0.957	1.095
	(0.105)	(0.042)	(0.041)	(0.041)	(0.043)	(0.037)	(0.149)	(0.132)	(0.140)
$PC_{a,3}$	−0.034	−0.110	−0.112	–	–	–	–	–	–
	(0.078)	(0.035)	(0.037)						
$PC_{a,4}$	0.069	0.039	–	–	–	–	−0.365	−0.328	−0.322
	(0.081)	(0.036)					(0.097)	(0.104)	(0.109)
const	1.834	1.851	1.850	1.850	1.859	1.859	1.259	1.186	1.186
	(0.080)	(0.038)	(0.038)	(0.042)	(0.041)	(0.036)	(0.094)	(0.113)	(0.126)
I_1	2.478	0.847	0.951	0.914	–	–	−4.080	–	–
	(0.856)	(0.210)	(0.222)	(0.231)			(0.409)		
I_2	−0.334	−0.171	−0.165	−0.209	–	–	−0.817	–	–
	(0.031)	(0.018)	(0.020)	(0.013)			(0.025)		
I_3	2.711	0.932	1.036	0.987	–	–	−5.440	–	–
	(0.872)	(0.219)	(0.232)	(0.242)			(0.538)		
Id_1	–	−0.266	−0.269	−0.277	−0.296	–	−0.354	−0.515	–
		(0.036)	(0.036)	(0.035)	(0.037)		(0.124)	(0.166)	
Id_2	–	0.469	0.465	0.439	0.454	–	–	–	–
		(0.038)	(0.036)	(0.038)	(0.038)				
R2	**0.843**	**0.957**	**0.956**	**0.950**	**0.947**	**0.816**	**0.867**	**0.799**	**0.753**
Adj R2	**0.837**	**0.955**	**0.954**	**0.949**	**0.946**	**0.813**	**0.862**	**0.794**	**0.748**
Var %	π	π	π	π	π	π	$€g$	$€g$	$€g$
$PC_{n,1}$	0.00	0.00	–	–	–	–	**0.18**	**0.16**	**0.16**
$PC_{n,2}$	**0.13**	**0.16**	**0.16**	**0.16**	**0.18**	**0.16**	–	–	–
$PC_{n,3}$	**0.04**	**0.05**	**0.05**	**0.04**	**0.04**	**0.04**	**0.05**	**0.05**	**0.05**
$PC_{n,4}$	**0.03**	**0.03**	**0.03**	**0.02**	**0.02**	**0.02**	**0.02**	**0.02**	**0.02**
$PC_{a,1}$	**0.35**	**0.27**	**0.27**	**0.27**	**0.28**	**0.39**	**0.10**	**0.14**	**0.20**
$PC_{a,2}$	**0.09**	**0.06**	**0.06**	**0.07**	**0.08**	**0.14**	**0.22**	**0.19**	**0.25**
$PC_{a,3}$	0.00	**0.01**	**0.01**	–	–	–	–	–	–
$PC_{a,4}$	0.00	0.00	–	–	–	–	**0.03**	**0.02**	**0.02**
Id_1	–	**0.04**	**0.04**	**0.04**	**0.04**	–	**0.03**	**0.06**	–
Id_2	–	**0.11**	**0.11**	**0.10**	**0.10**	–	–	–	–

The Table reports the results of the estimated PC regressions for the (demeaned) monthly headline inflation rate on selected standardized PCs extracted from the MLT ($PC_{n,i}$) and ST ($PC_{a,i}$) series. Figures in round brackets refer to Newey-West consistent SE. The (adjusted) coefficient of determination values is denoted as (***Adj R2***) ***R2.*** The Table also reports the % inflation variance accounted for by any of the selected PCs (***Var %***). The impulse dummy variables for the inflation equation are I_1:2022(6), I_2:2022(7) + 2022(6), I_3:2022(8) + 2022(7); for the output equation are I_1:2020(7) + 2020(6), I_2:2020(8) + 2020(7), I_3:2022(9) + 2022(8); The idiosyncratic components are $Id_1 : PC_{n,7}$, $Id_2 : PC_{n,9}$.

inflation (*STC*).

Moreover,

$$\pi_t^{nc} \equiv E\left[(\pi_t - \widehat{\mu}_\pi)\middle|\widehat{f}_{\mathbf{a}_1,t}, \widehat{f}_{\mathbf{a}_2,t}\right] = \widehat{\beta}_4 \widehat{f}_{\mathbf{a}_1,t} + \widehat{\beta}_5 \widehat{f}_{\mathbf{a}_2,t}, \tag{30}$$

where cyclical inflation (π_t^{nc}) measures the expected (demeaned) headline inflation conditional to the macro-financial information set subsumed by its short-term demand-side ($\widehat{\mathbf{f}}_{\mathbf{a}_1}$) and supply-side ($\widehat{\mathbf{f}}_{\mathbf{a}_2}$) components, respectively. Finally,

$$\begin{aligned} res_{\pi,t} \equiv\ & \pi_t - E\left[\pi_t \middle| \widehat{f}_{\mathbf{n}_2,t}, \widehat{f}_{\mathbf{n}3,t}, \widehat{f}_{\mathbf{n}_4,t}, \widehat{f}_{\mathbf{a}_1,t}, \widehat{f}_{\mathbf{a}_2,t}\right] \\ \equiv\ & \pi_t - \left(\widehat{\mu}_\pi + \widehat{\beta}_1 \widehat{f}_{\mathbf{n}_2,t} + \widehat{\beta}_2 \widehat{f}_{\mathbf{n}_3,t} + \widehat{\beta}_3 \widehat{f}_{\mathbf{n}_4,t} + \widehat{\beta}_4 \widehat{f}_{\mathbf{a}_1,t} + \widehat{\beta}_5 \widehat{f}_{\mathbf{a}_2,t}\right) \\ \equiv\ & \widehat{\beta}_6 \widehat{f}_{\mathbf{n}_7,t} + \widehat{\beta}_7 \widehat{f}_{\mathbf{n}_9,t} + \widehat{v}_{\pi,t} \\ \equiv\ & shock_{\pi,t} + \widehat{v}_{\pi,t}, \end{aligned} \tag{31}$$

where residual inflation ($res_{\pi,t}$) measures the unexpected inflation rate, given the information set composed by the common *MLT* and *ST* factors. The latter is the inflation rate shock $shock_{\pi,t}$, accounting for major idiosyncratic demand ($\widehat{\mathbf{f}}_{\mathbf{n}_7,t}$) and supply-side ($\widehat{\mathbf{f}}_{\mathbf{n}_9,t}$) tensions in the sample considered and further unaccounted inflationary pressures $\widehat{v}_{\pi,t}$, as also likely originated by Russia's war in Ukraine. In this respect, $res_{\pi,t}$ is, on average, about 1.4% from September 2021 through August 2022 and 2% from March through August 2022, while figures for $\widehat{v}_{\pi,t}$ are 0% and 0.3% (not reported).

As the PCA involves some transformed *MLT* variables, the orthogonality of the various components is not granted by construction. Sample correlations show that π_t^c and π_t^{nc} are near orthogonal (the correlation coefficient is 0.09 and not statistically different from zero at the 5% level); moreover, π_t^c and $res_{\pi,t}$ are fully orthogonal. Hence, in our context, no entrenching of demand and supply-side cyclical and residual inflations into core inflation is measured, consistent with our equilibrium/steady-state interpretation of core inflation. The core rate is determined by those trend supply-side and demand-side developments implicitly accommodated by monetary policy. On the other hand, some weak correlation can be found between π_t^{nc} and $shock_{\pi,t}$, i.e., 0.28, while both components are orthogonal to $\widehat{v}_{\pi,t}$. This finding is not surprising given the information content of $shock_{\pi,t}$.

Fig. 3 plots the historical decomposition of headline inflation into its

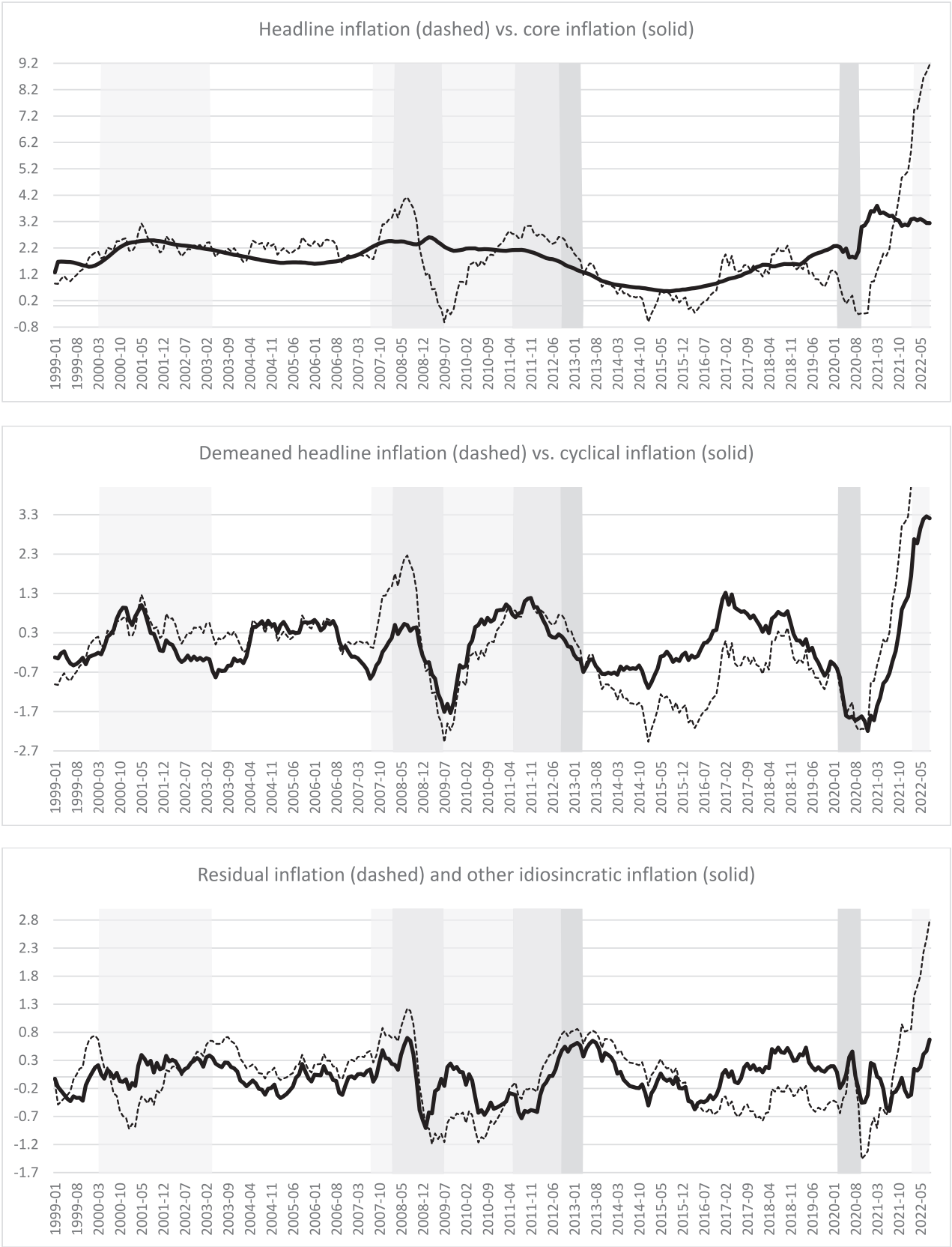

Fig. 3. Headline inflation decomposition in core (top plot), cyclical (center plot), and residual (bottom plot) components.

core (π_t^c), non-core (cyclical; π_t^{nc}), and residual ($res_{\pi,t}$ and $\widehat{v}_{\pi,t}$) components. For graphical convenience, we truncate the vertical axis in the center plot at a maximum of 3.5%. The top plot in Fig. 3 shows that the proposed structural core inflation measure is much smoother than headline inflation, well-tracking its underlying evolution. Our core inflation has been close to the 2% ECB reference value from 1999 through 2011. A persistent decline in core inflation occurred during the sovereign debt crisis recession and the associated recovery, down to about 0.6%. Starting in August 2015, likely due to the Q.E. policy initiated by the ECB in January 2015 and terminated in 2018, an upward trend can be noted in core inflation, achieving its 2% reference value by the end of 2019. While core inflation only weakly contracted during the pandemic recession, it rose much more sizably during the economic recovery through March 2021 (3.8%), to decline after that throughout the sample's end. The core inflation point estimate for August 2022 (the end of our sample) is 3.1%, with a regression standard error of 0.3% (not reported).

The decomposition also sheds light on two puzzles debated in the literature concerning "missing disinflation" during the Great Recession and "missing inflation" in its recovery phase (Bobeica & Jarocinski, 2019). As shown in the center and bottom plots in Fig. 3, residual inflation was the key driver of "excess inflation" during the early phase of the Great Recession. In contrast, cyclical inflation played a minor role. Then, cyclical inflation was the critical driver of reinflation during the recovery from the Great Recession through the beginning of the sovereign debt recession in 2011, while residual inflation was disinflationary over the same period. On the other hand, cyclical (and trend) weakness appears to be the most significant determinant of low inflation during the recovery from the sovereign debt recession through the end of 2015. Finally, cyclical inflation was the key driver of the disinflation during the pandemic recession, while both cyclical and residual components yielded a sizable contribution to the post-pandemic burst. Point estimates for August 2022 are 3.2% and 2.8% for cyclical and residual inflation, respectively. Overall, cyclical inflation tracks the disinflation during the three recessions in the sample and the reinflation during their recovery phase, but for the recovery from the sovereign debt crisis. Hence, we do not detect missing disinflation for any of the recessions in the sample. Moreover, we do not detect missing inflation during the recovery from the Great Recession and the pandemic recession. Yet, we find some missing inflation during the recovery from the sovereign debt recession.

5.1. Insights on core inflation drivers

STC is theoretically grounded on a widely accepted view of steady-state inflation determinants, affecting agents' expectations about the future course of inflationary developments. Given its definition and construction, *STC* fits the expected inflation rate component in a textbook Phillip's curve. Fig. 4 plots the historical decomposition of core inflation into its demand-side ($\widehat{\beta}_2\widehat{\mathbf{f}}_{\mathbf{n}_3} + \widehat{\beta}_3\widehat{\mathbf{f}}_{\mathbf{n}_4}$) and supply-side ($\widehat{\beta}_1\widehat{\mathbf{f}}_{\mathbf{n}_2}$) components. In the plots, we add the mean inflation rate $\widehat{\mu}_\pi$ to any of the components for graphical convenience. Fig. 5 plots a similar disentangling for the cyclical inflation component ($\widehat{\beta}_4\widehat{\mathbf{f}}_{\mathbf{a}_1} + \widehat{\beta}_5\widehat{\mathbf{f}}_{\mathbf{a}_2}$). As shown in Figure 4, top and center plots, supply-side core inflation is more volatile than demand-side core inflation, accounting for over two-thirds of overall core inflation variance (70% and 30%, respectively; not reported). Moreover, as shown in the bottom plot, the fiscal part ($\widehat{\beta}_2\widehat{\mathbf{f}}_{\mathbf{n}_3}$) dominates the monetary part ($\widehat{\beta}_3\widehat{\mathbf{f}}_{\mathbf{n}_4}$) of demand-side core inflation, accounting for over two-thirds of its variance (70% and 30%, respectively; not reported). The supply and demand-side components contributed to the disinflationary dynamics in the early 2000s. The core inflation surge in the mid-2000s was supply-side-driven, only partially offset by contrarian demand-side developments. Interestingly, the contrarian demand-side contribution was determined by its fiscal component, as the monetary part was inflationary from the mid-2000s through the early phase of the Great Recession.

On the other hand, both the demand and supply-side components account for the core inflation reversion during the Great Recession. While the supply-side core switched right at the beginning of the Great Recession, the demand-side core reversed halfway through the recession, much more abruptly after that. The temporary offsetting explains why the overall core inflation decline during the Great Recession accelerated at the end of the episode. The core inflation stabilization during the recovery period from the Great Recession through the sovereign debt crisis initial phase is the outcome of demand and supply-side components offsetting each other. Then, as the crisis turned into a recession, both parts similarly contributed to the core inflation decline to its minimum historical value of about 0.6%, scored in 2015. Since then, core inflation has been drifting upward. Both components have contributed to this upward trend, albeit the supply-side part to a more significant extent. Concerning the demand-side developments, as shown in Fig. 4, bottom plot, the contribution of the monetary component increased since the beginning of the Q.E. policy in early 2015, particularly during the most expansionary phase of the Q.E. policy from mid-2016 through mid-2017. Since the end of 2018, monetary core inflation has followed a steady decline as the Q.E. policy was phased out, only temporarily reversed during the Covid-19 recession when the ECB started the Pandemic Emergency Purchase Program (PEPP).[4] On the other hand, the fiscal component has been inflationary since 2017, also persisting throughout the pandemic recession.

In Fig. 6, we restrict the sample to 2019:1–2022:8 to better highlight inflation developments in the pandemic and post-pandemic periods. The top plot reports the decomposition of headline inflation into the core, non-core, and residual components. The upper center plot displays the demand-side (*core ds*) and supply-side (*core ss*) core parts. The lower center plot displays the demand-side (*non-core ds*) and supply-side (*non-core ss*) cyclical parts. The bottom plot reports the idiosyncratic demand-side ($shock_\pi$ *ds*), supply-side ($shock_\pi$ *ss*), and other (v_π) residual parts. As shown in Fig. 6, top and upper center plots, the core inflation overall upward trend temporarily reversed during the pandemic recession due to the sizable supply-side contraction, only partially offset by the (monetary and fiscal) demand-side expansions. Core inflation anticipated cyclical and headline inflation in the post-pandemic recovery period (top plot). Supply-side core inflation trended upward from September 2020 through March 2021, then slightly declined through January 2022 and increased again since February 2022 (upper center plot). On the other hand, demand-side core inflation has been on a persistent downward trend, offsetting supply-side dynamics since February 2022, accounting for the slight decline in core inflation since the beginning of Russia's war in Ukraine (upper center plot). The core inflation rate at the end of our sample (August 2022) is about one percentage point above the target, at 3.1% (top plot).

5.2. Insights on cyclical inflation drivers

Fig. 5 plots the historical decomposition of cyclical inflation into its demand-side ($\widehat{\beta}_4\widehat{\mathbf{f}}_{\mathbf{a}_1}$) and supply-side ($\widehat{\beta}_5\widehat{\mathbf{f}}_{\mathbf{a}_2}$) components. As shown in Fig. 5, the volatility of cyclical inflation is primarily accounted for by its

[4] The Q.E. policy was started in January 2015 and terminated in December 2018. Monthly asset purchases averaged €60 billion from March 2015 to March 2016; €80 billion from April 2016 to March 2017; €60 billion from April 2017 to December 2017; €30 billion from January 2018 to September 2018; €15 billion from October 2018 to December 2018. Asset purchases restarted at a monthly pace of €20 billion in November 2019. A new Q.E. policy started in March 2020, i.e., the pandemic emergency purchase program (PEPP), consisting of additional monthly net asset purchases of €120 billion through the end of 2020, to face the adverse effects of the pandemic. The ECB increased the PEPP by €500 billion to €1,850 billion in December 2020 and extended it through March 2022.

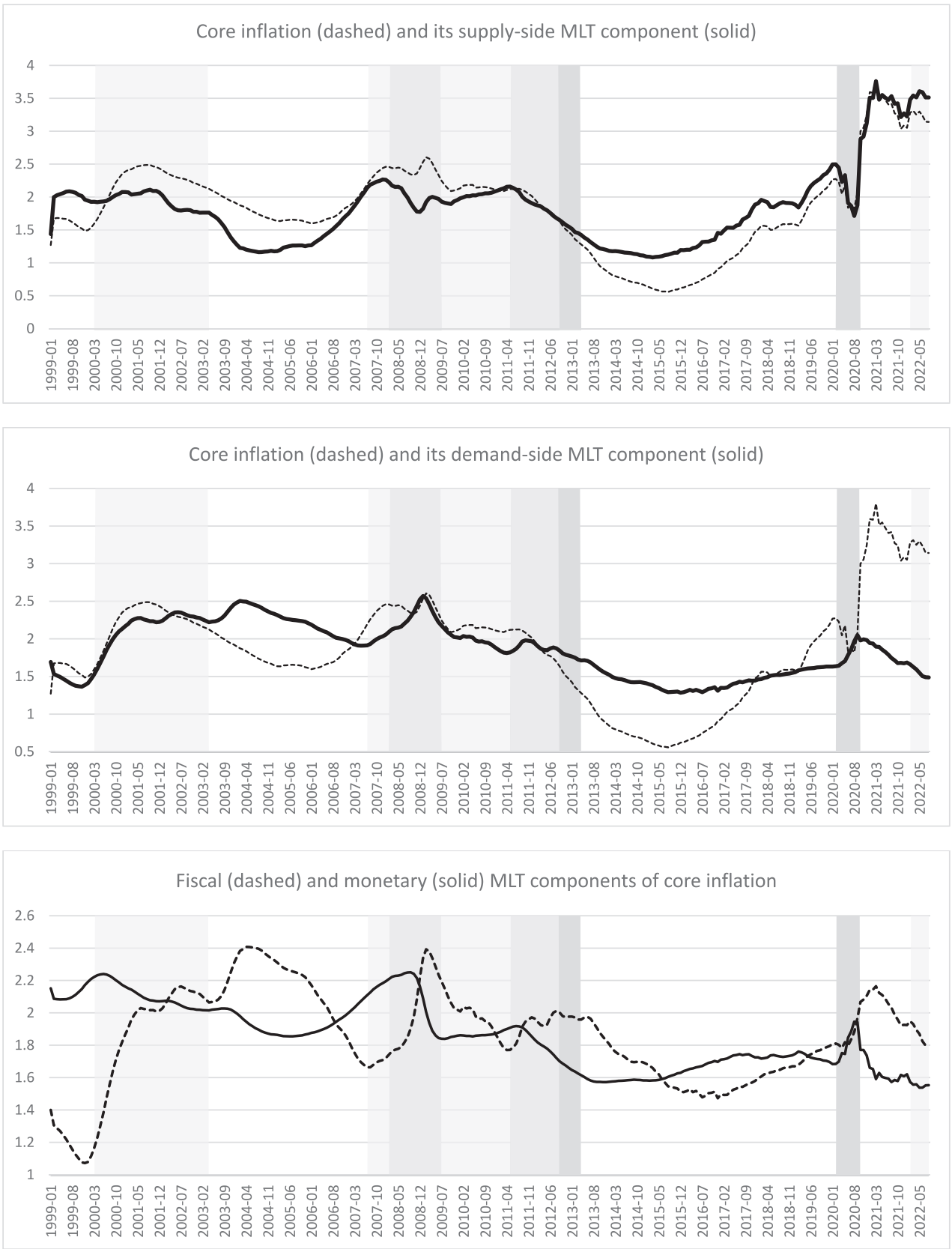

Fig. 4. Core inflation decomposition in the persistent supply-side (top plot) and demand-side (center and bottom plots) components.

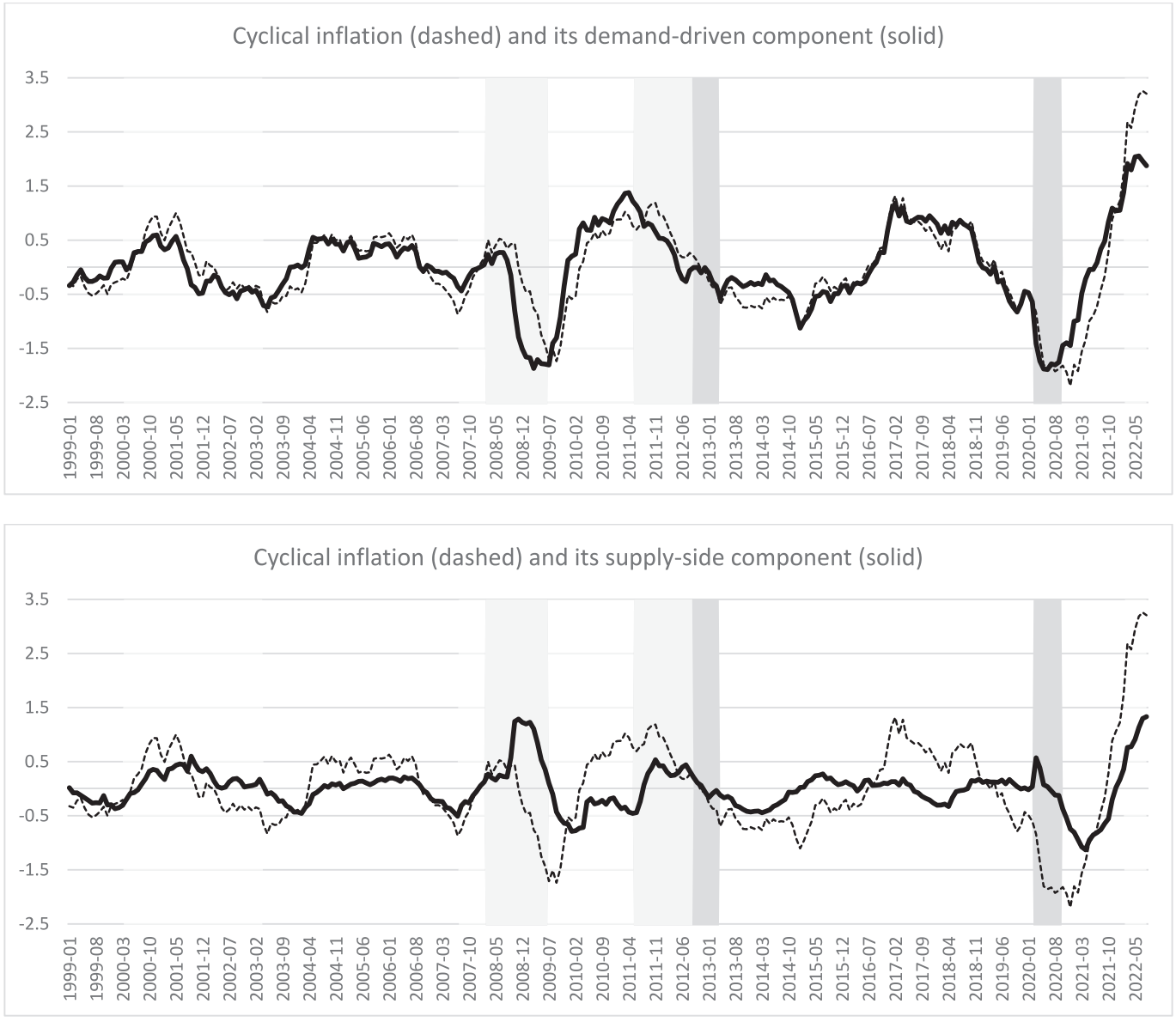

Fig. 5. Cyclical inflation decomposition in the supply-side (top plot) and demand-side (bottom plot) components.

demand component ($\widehat{\beta}_4\widehat{\mathbf{f}}_{\mathbf{a}_1}$: 80%; $\widehat{\beta}_5\widehat{\mathbf{f}}_{\mathbf{a}_2}$: 20%; not reported). During the stock market crisis in the early 2000s, supply and demand-side cyclical inflations were disinflationary with coincidental timing. A different pattern emerged during the subprime financial crisis and the Great Recession. The supply-side component accounts almost entirely for the upsurge in cyclical inflation from the inception of the financial crisis halfway through the Great Recession. On the other hand, the demand-side component anticipates the headline inflation contraction occurring in the second half of the Great Recession period and the upsurge during the recovery and initial phases of the sovereign debt crisis. As the recession sets in, the demand-side component contributes to and anticipates the disinflationary drift in cyclical inflation, while the supply-side part shows the opposite behavior. The inflation hiatus detected during the recovery from the post-sovereign debt recession (2013:10–2016:11) is largely demand-driven, albeit a supply-side contribution is noted through 2014. The demand-side component is also the chief driver of the 2016–2018 cyclical inflation surge (the period in which the ECB Q.E. policy was strongest). As shown in Fig. 6, lower center plot, both cyclical inflation components have declined during the pandemic recession. The demand-side component has then led the rise in the supply-side component of about seven months, increasing since October 2020. Inflationary pressure in the post-pandemic recession recovery period is then mainly contributed by cyclical and residual inflation (top plot). Interestingly, cyclical inflation appears to have stabilized since June 2022 due to the offsetting impact of cyclical demand-side inflation on cyclical supply-side inflation (lower center plot). In contrast, residual inflation appears to be a persistent source of inflationary pressure in the euro area, particularly the supply-side part, coherent with its association with supply-chain and energy price developments and further geopolitical tensions (bottom plot). As of August 2022, cyclical and residual inflation yield a similar contribution to headline inflation, contributing 3.2% and 2.8%, respectively. Concerning cyclical inflation, the demand-side component shows the largest contribution, i.e., 1.9% versus 1.3% for the supply-side component. Concerning residual inflation, the supply-side component (energy and supply chain) shows the largest contribution, i.e., 1.6% versus 0.5% for the demand-side component. Other price tensions, possibly arising from current geopolitical stress, account for 0.7%.

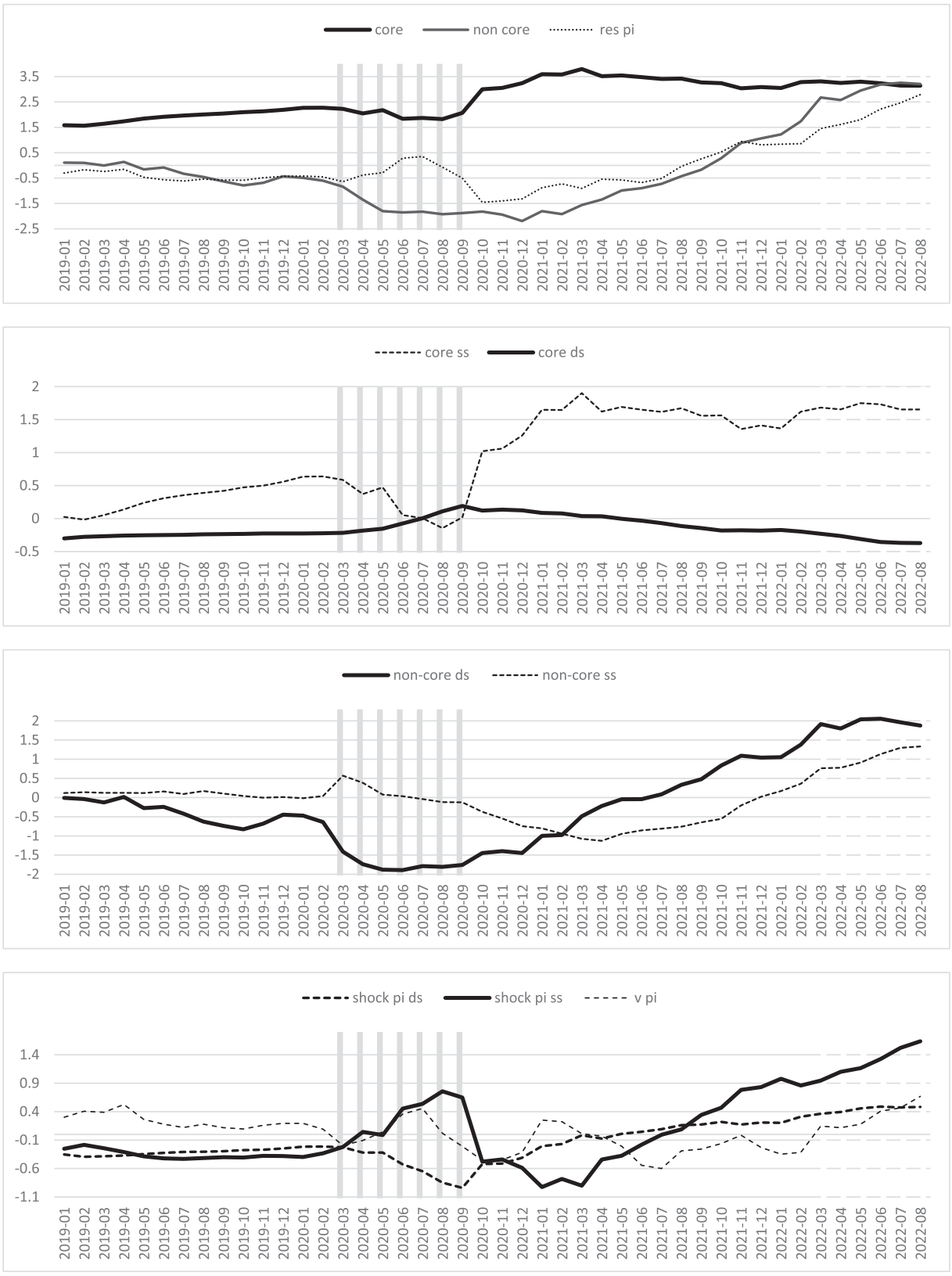

Fig. 6. Recent inflation developments: demand-side and supply-side core, cyclical and residual components.

6. Policy implications

Headline inflation appears currently evenly determined by its core, cyclical, and residual components, i.e., about 3% each (Fig. 6, top plot). Notwithstanding the inflationary pressure, ECB monetary policy has successfully mitigated the rise in core inflation, as the current deviation is estimated at one percent above its target level. Cyclical inflation and residual inflation are equally sizable headline inflation components, and the recent ECB interest rate hikes go in the direction of weakening the demand-side cyclical part.[5] However, the latter might also slow down autonomously due to the worsening economic outlook generated by Russia's war in Ukraine. In light of recent inflation developments and ECB interest rate hikes, we assess short and medium-term output growth prospects to gauge further evidence of the emergence of a stagflationary scenario. We report the results of the PC-regression analysis for the €-coin GDP growth rate in the last three columns of Table 5. The augmented model (column 7), retaining three composite impulse dummy variables accounting for the depth of the pandemic recession (June to September 2020) and the idiosyncratic demand-side component $\widehat{\mathbf{f}}_{\mathbf{n}_7}$, accounts for about 85% of output variance. It yields a 5% improvement relative to the model that omits the impulse dummy variables (column 8) and a 10% improvement relative to the model that includes only common components (column 9). The components of interests are then

$$MLT_{g,t} \equiv E\left[\epsilon g_t | \widehat{f}_{\mathbf{n}_1,t}, \widehat{f}_{\mathbf{n}_3,t}, \widehat{f}_{\mathbf{n}_4,t}\right] = \widehat{\mu}_{\epsilon g} + \widehat{\beta}_1 \widehat{f}_{\mathbf{n}_1,t} + \widehat{\beta}_2 \widehat{f}_{\mathbf{n}_3,t} + \widehat{\beta}_3 \widehat{f}_{\mathbf{n}_4,t}, \tag{32}$$

that yields information on medium to long-term GDP growth prospects, as accounted by developments along the financial cycle ($\widehat{\mathbf{f}}_{\mathbf{n}_1}$), plus persistent output developments determined by monetary ($\widehat{\mathbf{f}}_{\mathbf{n}_4}$) and fiscal policy ($\widehat{\mathbf{f}}_{\mathbf{n}_3}$);

$$ST_{g,t} \equiv E\left[\epsilon g_t | \widehat{f}_{\mathbf{a}_1,t}, \widehat{f}_{\mathbf{a}_2,t}, \widehat{f}_{\mathbf{a}_4,t}\right] = \widehat{\beta}_4 \widehat{f}_{\mathbf{a}_1,t} + \widehat{\beta}_5 \widehat{f}_{\mathbf{a}_2,t} + \widehat{\beta}_6 \widehat{f}_{\mathbf{a}_4,t}, \tag{33}$$

that yields information on short-term GDP growth prospects, as accounted by cyclical developments determined by short-term demand-side ($\widehat{\mathbf{f}}_{\mathbf{a}_1}$), supply-side ($\widehat{\mathbf{f}}_{\mathbf{a}_2}$) and financial ($\widehat{\mathbf{f}}_{\mathbf{a}_4}$) factors. Finally,

$$\begin{aligned} res_{g,t} \equiv\ & \epsilon g_t - E\left[\epsilon g_t | \widehat{f}_{\mathbf{n}_1,t}, \widehat{f}_{\mathbf{n}3,t}, \widehat{f}_{\mathbf{n}_4,t}, \widehat{f}_{\mathbf{a}_1,t}, \widehat{f}_{\mathbf{a}_2,t}, \widehat{f}_{\mathbf{a}_4,t}\right] \\ \equiv\ & \epsilon g_t - \left(\widehat{\mu}_{\epsilon g} + \widehat{\beta}_1 \widehat{f}_{\mathbf{n}_1,t} + \widehat{\beta}_2 \widehat{f}_{\mathbf{n}_3,t} + \widehat{\beta}_3 \widehat{f}_{\mathbf{n}_4,t} + \widehat{\beta}_4 \widehat{f}_{\mathbf{a}_1,t} + \widehat{\beta}_5 \widehat{f}_{\mathbf{a}_2,t} + \widehat{\beta}_6 \widehat{f}_{\mathbf{a}_4,t}\right) \\ \equiv\ & \widehat{\beta}_7 \widehat{f}_{\mathbf{n}_7,t} + \sum_{i=1}^{3} \widehat{\delta}_i I_{i,t} + \widehat{v}_{g,t} \\ \equiv\ & shock_{g,t} + \widehat{v}_{g,t}, \end{aligned}$$

where the residual output growth $res_{g,t}$ measures the unexpected GDP growth rate, given the information set composed by the common *MLT* and *ST* factors. The sum of the output rate shock $shock_{g,t}$ and the additional unaccounted (other) output developments $\widehat{v}_{g,t}$. $res_{g,t}$ accounts for major idiosyncratic demand-side tensions ($\widehat{\mathbf{f}}_{\mathbf{n}_7}$), as arose during the Great Recession and the pandemic recession, and further exogenous tensions during the pandemic recession (lock-down/containment impulse dummies).

We plot the $MLT_{g,t}, ST_{g,t}$ and $res_{g,t}$ indicators in Fig. 7, top plot. Moreover, we report the historical decomposition for the $MLT_{g,t}$and $ST_{g,t}$ components in the upper and lower center plots and for $res_{g,t}$ in the bottom plot. In the decomposition for $MLT_{g,t}$ in the upper center plot, we denote the financial cycle contribution $\widehat{\beta}_1 \widehat{f}_{\mathbf{n}_1,t}$ as MLT_g *fc*; the fiscal policy contribution $\widehat{\beta}_2 \widehat{f}_{\mathbf{n}3,t}$ as MLT_g *fp*; the monetary policy contribution $\widehat{\beta}_3 \widehat{f}_{\mathbf{n}_4,t}$ as MLT_g *mp*. Moreover, in the decomposition for $ST_{g,t}$ in the lower center plot, we denote the demand-side contribution $\widehat{\beta}_4 \widehat{f}_{\mathbf{a}_1,t}$ as ST_g *ds*; the supply-side contribution $\widehat{\beta}_5 \widehat{f}_{\mathbf{a}2,t}$ as ST_g *ss*; the financial contribution $\widehat{\beta}_6 \widehat{f}_{\mathbf{a}_4,t}$ as ST_g *fin*. For graphical convenience, we truncate the vertical axis in the top and bottom plots at a minimum of −3.5%. In light of the aim of the exercise, we restrict the sample to the period 2019:1–2022:8.

The top and upper center plots show that the pandemic recession did not negatively impact trend GDP prospects. The favorable development of the financial cycle in the face of the prompt implementation of the countercyclical fiscal-monetary policy mix likely accounts for this finding. The economic policy contribution to medium to long-term prospects weakens in the early recovery period. Since March 2021, the medium-term monetary policy contribution has stabilized at about −0.5%; on the other hand, consistent with the active implementation of the National Recovery and Resilience Plans, an upward trend in the medium-term fiscal policy contribution can be noted, achieving 0.1% in August 2022. As of August 2022, GDP growth in the euro area is 1.5% as of January 2020. This result is the outcome of the financial cycle contribution (0.5%) offsetting the demand-side contribution (-0.4%). As shown in the lower center and bottom plots, the pandemic contraction was largely cyclical, contributed by demand-side and supply-side factors. Its depth, triggered by lock-down and containment measures, is well captured by the exogenous $shock_{g,t}$ component. Following the deep pandemic contraction, short-term prospects gained momentum starting in October 2020 and peaked in April 2021 at about 2.2%. Beginning in November 2021, a progressive worsening led to a negative short-term outlook from March to April 2022. In August 2022, cyclical prospects were at −2.2%. This result is the outcome of a joint improvement in cyclical demand and supply side conditions since October 2020; while cyclical demand-side conditions kept improving, peaking at 1.9% in June 2022 and weakening to 1.7% in August 2022, cyclical supply-side conditions showed a steady worsening since May 2021, landing at −3.5% in August 2022. Moreover, the contribution of short-term financial factors is currently about −0.4%.

Our results suggest that ECB monetary policy has successfully mitigated the rise in core inflation above the target, postponing interest rates hiking and preserving macro-financial stability. Core inflation stickiness since early 2021 is the outcome of a stabilizing supply-side core partially offset by disinflationary demand-side (monetary and fiscal) inflation, consistent with the phasing out of the PEPP program and the fiscal stance turning neutral. The recent inflation uprise is short-term and largely supply-side driven. The eventual interest rate hike sequence started in July 2022 is also justified in light of keeping anchored households, firms, and financial market expectations.

Although the assessment is preliminary, we detect emerging stagflationary conditions driven by adverse short-term supply-side developments. A weakening of overall financial conditions ahead is also not excluded, as historical experience shows that the peak of the financial cycle likely occurs in a fairly flat region. If anything, a provisional turning point could be dated already in December 2020.

A pressing issue for ECB monetary policy will be to face inflationary pressure without triggering a financial crisis. Tensions from the ECB interest rate hikes have become manifest with Credit Suisse and Deutsche Bank turmoils in spring 2023. As generalized real wage increases are resisted, second-round effects of the current energy shock might be cushioned. Yet, supply-side factors are not under the ECB's control and are likely candidates for further inflationary pressure if the energy crisis persists and the EU energy policy remains unchanged. Provisions such as a price cap for oil and natural gas might provide temporary relief, conditional to more structural reforms being undertaken, coherent with the green transition detailed in the EU Green New Deal. Further price pressure can originate from food prices due to Russia's weaponization of some agricultural commodities and nearshoring/friendshoring policies to weaken dependence on Chinese supplies.

[5] The ECB raised its MRO rate to 0.5% on 27 July 2022, 1.25% on 14 September 2022, 2% on 2 November 2022, 2.5% on 21 December 2022, 3% on 8 February 2023, 3.50% on 22 March 2023, 3.75% on 10 May 2023, 4.0% on 21 June 2023, 4.25% on 2 August 2023.

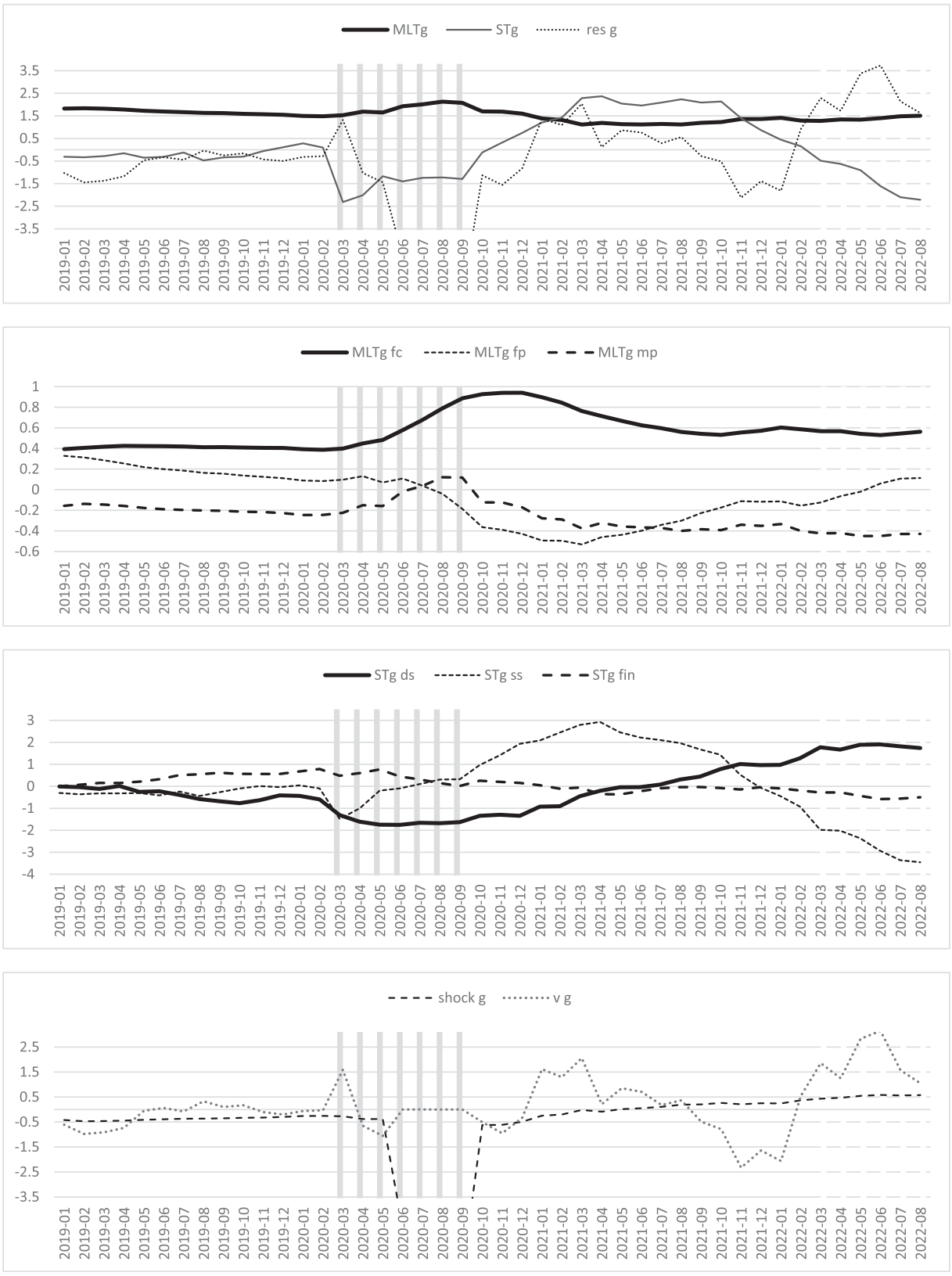

Fig. 7. Recent output developments: demand-side and supply-side MLT, ST, and residual components.

Weaker growth, higher policy interest rates, rising sovereign risk premia, and lack of fiscal capacity are all factors that can destabilize the euro area sovereign debt market. This is also in the light that the European response to the energy crisis will entail transfer payments and tax cuts, increasing public deficits. Also, the current geopolitical crisis will require public investment to support increased defense spending, putting further pressure on national balances unless differently funded. Moreover, by raising debt services, anti-inflationary monetary policies

might trigger insolvencies, falling asset prices, credit shortages, and eventually impair real activity. The risk of a financial boost is high, also in light of the prevailing high private and public debt ratios.

An extension of the Next Generation EU scope to face the energy crisis triggered by Russia's war in Ukraine and the current geopolitical crisis and cushion their stagflationary impact appears essential to grant resilience to the euro area. Due to the nature and origin of the threats, the conditions for such an extension appear to be available. This will prevent further pressure on national balances and add a fiscal policy tool to the existing monetary policy tools, such as the Outright Monetary Transactions and the Transactions Protection Instrument, to navigate the current unprecedented energy and geopolitical crisis. As entailed in the National Plans for Recovery and Resilience, a deepening of growth-oriented supply-side policies, fostering green investment and energy-saving technology, is an exemplification of what is needed to counteract the sequence of left-ward shifts in the short-run aggregate supply schedule we can expect to persist over the near future. This also appears viable in light of the negative and negligible (estimated) contribution of medium to long-term fiscal inflation to core inflation.

7. Structural core inflation properties

Beyond theoretical grounding and economic interpretability, a core inflation measure should display some desirable properties (Bryan & Cecchetti, 1994; Wynne, 2008). First, the estimated core inflation series should act as a trend for headline inflation, showing lower variability and higher persistence. Second, it should possess forecasting power for headline inflation. Third, it should be robust to sample updating to act as an external information source. This latter property is not met by measures obtained from econometric procedures, for which new observations may entail changes in past core inflation figures, making them more of an internal tool of inflation analysis for monetary policy than a source for external communication. Hence, below, we focus on the former two properties.

7.1. Trend and smoothness properties

In Table 6, we report descriptive statistics for the structural core inflation rate (*STC*), the headline HICP inflation rate (HICP), and the Ex-Food and Energy HICP inflation rate (EXFE). For comparison, we also report descriptive statistics for various available core inflation measures routinely used at the ECB for internal evaluation, i.e., the Supercore (SUP), the Persistent and Common Component of Inflation (PCC), the Persistent and Common Component of Inflation computed using EXFE (PCC2), the Trimmed Mean inflation rate with 10% and 30% symmetric trimming (TR10, TR30), the Weighted Median inflation rate (WMED). The latter core inflation measures are available from the ECB Statistical Data Warehouse. As shown in Panel A, all the core inflation measures are sizably smoother than the headline inflation rate. The *STC* volatility is about half of the volatility of the headline inflation rate, similar to SUP, PCC, TR30, and WMED. EXFE and PCC2 are smoother, while TR10 is the most volatile core inflation rate. The same results hold for the core inflation measures in changes. Yet, in this latter case, the *STC* volatility is just about a third of the volatility of the headline inflation rate and about half of the volatility of the other core measures, apart from PCC2.

All the core inflation measures are positively correlated between them and with headline inflation. The sample correlation coefficients for all series but *STC* are in the range [0.85–0.96]; on the other hand, the correlation coefficient of the various series with *STC* is lower, in the range [0.46–0.61], suggesting that *STC* might contain additional information on trend inflation dynamics relative to the other measures. This finding is even more evident from the correlation coefficients computed for the series in differences. The correlation of headline inflation with *STC* is only 0.09, while it is in the range [0.40–0.66] for the other core measures.

7.2. Forecasting properties

The forecasting power of our core inflation measure is theoretically warranted by its definition in terms of conditional headline inflation expectation, given relevant information on medium to long-term demand-side and supply-side developments. We assess this property in-sample and out-of-sample. A first exercise requires estimating a bivariate error correction model, including the headline and core inflation rates. Within this context, we assess both Granger-causality and error-correction properties. Ideally, headline inflation should be Granger-caused by core inflation and correct its gap relative to the core rate, i.e., it should mean-revert toward the core inflation rate. Moreover, the core inflation rate should neither be Granger-caused by headline inflation nor error-correcting. This outcome would suggest the usefulness of

Table 6
Descriptive statistics for the various core inflation measures and headline inflation.

Panel A: Sample Means and Standard Deviations

	SUP	PCC	PCC2	TR10	TR30	WMED	EXFE	*STC*	HICP
MEAN (level)	1.58	1.87	1.41	1.77	1.65	1.65	1.36	1.82	1.83
ST DV (level)	0.70	0.81	0.34	1.17	0.85	0.79	0.58	0.73	1.52
MEAN (change)	0.01	0.01	0.00	0.02	0.02	0.02	0.01	0.00	0.03
ST DV (change)	0.14	0.15	0.05	0.22	0.17	0.19	0.22	0.09	0.31

Panel B: Sample correlation coefficients for levels (below diagonal) and changes (above diagonal)

	SUP	PCC	PCC2	TR10	TR30	WMED	EXFE	*STC*	HICP
SUP		0.21	0.25	0.61	0.73	0.61	0.79	**0.08**	**0.55**
PCC	0.85		0.93	0.44	0.23	0.15	0.18	**0.05**	**0.48**
PCC2	0.89	0.95		0.40	0.26	0.17	0.20	**0.04**	**0.40**
TR10	0.92	0.91	0.88		0.78	0.60	0.57	**0.15**	**0.86**
TR30	0.94	0.85	0.85	0.98		0.78	0.63	**0.16**	**0.65**
WMED	0.95	0.86	0.86	0.96	0.99		0.51	**0.07**	**0.50**
EXFE	0.96	0.83	0.86	0.90	0.92	0.92		**0.10**	**0.55**
STC	**0.47**	**0.59**	**0.61**	**0.54**	**0.52**	**0.52**	**0.48**		**0.09**
HICP	**0.86**	**0.91**	**0.88**	**0.98**	**0.93**	**0.91**	**0.85**	**0.53**	

The Table reports descriptive statistics for various core inflation measures and the HICP headline inflation rate in levels and changes. Panel A reports the sample mean (MEAN) and standard deviations (ST DEV). Panel B reports the sample correlation coefficients. The series are the Super Core rate (SUP), the Persistent and Common Component rate (PCC), the Persistent and Common Component rate computed using the ex-food and energy inflation rate (PCC2), the Trimmed mean inflation rate with 10% and 30% symmetric trimming (TR10, TR30), the weighted median inflation rate (WMED), the ex-food and energy inflation rate (EXFE), the Structural Core rate (*STC*), and the headline HICP rate (HICP).

Table 7
Granger-Causality and Error-Correction tests.

Panel A: Granger-Causality tests

	Caused Variables								
Causal Variables	**SUP**	**PCC**	**PCC2**	**TR10**	**TR30**	**WMED**	**EXFE**	***STC***	**HICP**
HICP	**[0.0495]**	**[0.0224]**	**[0.0039]**	**[0.0018]**	**[0.0312]**	[0.0724]	[0.0811]	[0.1791]	
	[0.0295]	**[0.0091]**	**[0.0023]**	**[0.0037]**	**[0.0436]**	[0.1243]	[0.0583]	[0.6407]	
STC	**[0.0033]**	**[0.0000]**	**[0.0000]**	**[0.0010]**	**[0.0000]**	**[0.0000]**	**[0.0005]**		**[0.0048]**
	[0.0000]	**[0.0000]**	**[0.0000]**	**[0.0003]**	**[0.0000]**	**[0.0000]**	**[0.0182]**		**[0.0491]**

	Causal Variables								
Caused Variables	**SUP**	**PCC**	**PCC2**	**TR10**	**TR30**	**WMED**	**EXFE**	***STC***	**HICP**
HICP	[0.1304]	**[0.0000]**	**[0.0002]**	[0.0524]	**[0.0036]**	[0.2053]	[0.0938]	**[0.0048]**	
	[0.1534]	**[0.0001]**	**[0.0002]**	[0.0986]	**[0.0247]**	[0.0673]	**[0.0027]**	**[0.0491]**	
STC	[0.1497]	**[0.0179]**	[0.6032]	**[0.0489]**	[0.1385]	[0.3617]	**[0.0015]**		[0.1791]
	[0.2032]	**[0.0059]**	[0.4569]	[0.2500]	[0.2557]	[0.6543]	[0.3143]		[0.6407]

Panel B: Error-Correction tests

	Caused Variables								
Causal Variables	**SUP**	**PCC**	**PCC2**	**TR10**	**TR30**	**WMED**	**EXFE**	***STC***	**HICP**
HICP	[0.5149]	**[0.0084]**	**[0.0210]**	[0.8613]	[0.2401]	[0.0726]	[0.3104]	[0.1031]	
	[0.4352]	**[0.0038]**	**[0.0218]**	[0.8307]	[0.2035]	[0.0531]	[0.3124]	[0.3042]	
STC	**[0.0047]**	**[0.0123]**	[0.1752]	**[0.0004]**	**[0.0000]**	**[0.0000]**	**[0.0124]**		[0.0766]
	[0.0083]	**[0.0130]**	[0.1486]	**[0.0018]**	**[0.0004]**	**[0.0000]**	**[0.0274]**		[0.0766]

	Causal Variables								
Caused Variables	**SUP**	**PCC**	**PCC2**	**TR10**	**TR30**	**WMED**	**EXFE**	***STC***	**HICP**
HICP	[0.0592]	**[0.0197]**	[0.1615]	[0.0860]	[0.1137]	[0.0930]	[0.3033]	[0.0766]	
	[0.0493]	**[0.0266]**	[0.1821]	[0.0666]	[0.0945]	[0.0724]	[0.3201]	[0.0766]	
STC	[0.8914]	[0.4063]	[0.3343]	**[0.0373]**	[0.1478]	[0.3786]	[0.9864]		[0.1031]
	[0.9421]	[0.5166]	[0.3993]	[0.2519]	[0.4486]	[0.5988]	[0.9917]		[0.3042]

Panel C: Joint Granger-Causality and Error-Correction tests

	Caused Variables								
Causal Variables	**SUP**	**PCC**	**PCC2**	**TR10**	**TR30**	**WMED**	**EXFE**	***STC***	**HICP**
HICP	**[0.0051]**	**[0.0224]**	**[0.0060]**	**[0.0025]**	**[0.0009]**	**[0.0002]**	**[0.0031]**	[0.1508]	
	[0.0016]	**[0.0052]**	**[0.0038]**	**[0.0049]**	**[0.0013]**	**[0.0020]**	**[0.0054]**	[0.6208]	
STC	**[0.0001]**	**[0.0000]**	**[0.0000]**	**[0.0000]**	**[0.0000]**	**[0.0000]**	**[0.0000]**		**[0.0048]**
	[0.0000]	**[0.0000]**	**[0.0000]**	**[0.0000]**	**[0.0000]**	**[0.0000]**	**[0.0151]**		**[0.0491]**

	Causal Variables								
Caused Variables	**SUP**	**PCC**	**PCC2**	**TR10**	**TR30**	**WMED**	**EXFE**	***STC***	**HICP**
HICP	[0.0792]	**[0.0000]**	**[0.0001]**	**[0.0071]**	**[0.0023]**	[0.1699]	[0.1168]	**[0.0048]**	
	[0.0618]	**[0.0000]**	**[0.0000]**	**[0.0112]**	**[0.0068]**	**[0.0408]**	**[0.0042]**	**[0.0491]**	
STC	[0.1837]	**[0.0247]**	[0.5732]	**[0.0339]**	[0.1207]	[0.3672]	**[0.0019]**		[0.1508]
	[0.0476]	**[0.0037]**	**[0.0241]**	[0.2595]	[0.2822]	[0.6529]	[0.0699]		[0.6208]

The Table reports p-values for the Wald-tests for Granger-causality for the core inflation measures and actual headline inflation. Panel A reports the results of the joint hypotheses *i*) and *iv*), Panel B for hypotheses *ii*) and *v*), and Panel C for hypotheses *iii*) and *vi*). The distribution of the tests is $\chi^2_{(df)}$, where $df = 12$ for the tests in *i*) and *iv*), $df = 1$ for the tests in *ii*) and *v*), $df = 13$ for the tests in *iii*) and *vi*). For each case, we report results using the OLS Variance-Covariance matrix (upper square parenthesis) and the White heteroskedasticity-consistent Variance-Covariance matrix (lower square parenthesis). Figures in bold highlight the rejection of the null hypothesis at the 5 % significance level. For instance, in line 1, column 1, in Panel A, we report the p-values for the tests of Granger non-causality of headline inflation for Supercore; [0.0495] is obtained using the OLS Var-Cov matrix, [0.0295] is obtained using the White Heteroskedasticity-consistent Var-Cov matrix. Hence, in both cases, the null hypothesis that headline inflation is not Granger-causing Supercore is rejected at the 5 % level. On the other hand, in line 4, column 1, in Panel A, we report the p-values for the tests of Granger non-causality of the Supercore inflation rate for headline inflation; [0.1304] is obtained using the OLS Var-Cov matrix, [0.1534] is obtained using the White Heteroskedasticity-consistent Var-Cov matrix. Hence, in both cases, the null hypothesis that the Supercore rate is not Granger-causing the headline inflation rate is not rejected. The series are the Supercore (SUP), the Persistent and Common Component of Inflation (PCC), the Persistent and Common Component of Inflation computed using the Ex-Food and Energy inflation rate (PCC2), the Trimmed Mean inflation rate with 10 % and 30 % symmetric trimming (TR10, TR30), the Weighted Median inflation rate (WMED), the Ex-Food and Energy inflation rate (EXFE), the Structural Core rate (*STC*), and the headline HICP rate (HICP).

the core inflation measure for headline inflation forecasting, pointing to the information sufficiency of the core inflation measure relative to the non-core inflation component (Freeman, 1998). Moreover, it implies no pass-through of cyclical inflation into core inflation, consistent with an equilibrium/steady-state interpretation of core inflation.

Hence, the model is

$$\begin{aligned}\Delta\pi_t = &\quad \alpha_1 + \sum_{j=1}^{p}\gamma_{1,j}\Delta\pi_{t-j} + \sum_{j=1}^{p}\delta_{1,j}\Delta\pi^c_{t-j} + \beta_1\left(\pi_{t-1} - \pi^c_{t-1}\right) + \varepsilon_{1,t}\\ \Delta\pi^c_t = &\quad \alpha_2 + \sum_{j=1}^{p}\gamma_{2,j}\Delta\pi_{t-j} + \sum_{j=1}^{p}\delta_{2,j}\Delta\pi^c_{t-j} + \beta_2\left(\pi_{t-1} - \pi^c_{t-1}\right) + \varepsilon_{2,t},\end{aligned} \tag{34}$$

and the relevant hypotheses to be tested are

(*i*) headline inflation is not Granger-caused by core inflation $H_0 : \delta_{1,1} = \delta_{1,2} = \ldots = \delta_{1,p} = 0$ vs. $H_1 : H_0$ is false;

(*ii*) headline inflation is not error-correcting relative to core inflation (π_t is weakly exogenous) $H_0 : \beta_1 = 0$ vs. $H_1 : H_0$ is false;

(*iii*) headline inflation is neither Granger-caused by core inflation nor error-correcting (π_t is strongly exogenous) $H_0 : \delta_{1,1} = \delta_{1,2} = \ldots = \delta_{1,p} = \beta_1 = 0$ vs. $H_1 : H_0$ is false.

Moreover,

(*iv*) core inflation is not Granger-caused by headline inflation $H_0 : \gamma_{2,1} = \gamma_{2,2} = \ldots = \gamma_{2,p} = 0$ vs. $H_1 : H_0$ is false;

(*v*) core inflation is not error-correcting relative to headline inflation (π^c_t is weakly exogenous) $H_0 : \beta_2 = 0$ vs. $H_1 : H_0$ is false;

(*vi*) core inflation is neither Granger-caused by headline inflation nor error-correcting (π^c_t is strongly exogenous) $H_0 : \gamma_{2,1} = \gamma_{2,2} = \ldots = \gamma_{2,p} = \beta_2 = 0$ vs. $H_1 : H_0$ is false.

A desirable core inflation measure would show rejection of the null hypothesis in *i*) through *iii*) and non-rejection of the null hypothesis in *iv*) through *vi*). We perform the same tests also to assess the *STC* excess information relative to the other core inflation measures. Concerning the ECM model in (34), the headline inflation variable π_t is then replaced by an alternative core inflation measure to *STC*. In this context, we would expect *STC* to Granger-cause the other core inflation measures and not show error-correcting properties, i.e., to show strong exogeneity, while the other measures are Granger-caused and error-correcting relative to *STC*.

In Table 7, we report the results of the Granger-causality tests allowing one-year adjustment dynamics ($p = 12$). In Panel A, we report the results of the joint hypotheses (*i*) and (*iv*), in Panel B for hypotheses (*ii*) and (*v*), and in Panel C for hypotheses (*iii*) and (*vi*). The distribution of the tests is χ^2_{df}, where $df = 12$ for the tests in (*i*) and (*iv*), $df = 1$ for the tests in (*ii*) and (*v*), and $df = 13$ for the tests in (*iii*) and (*vi*). For each case, we report results using the OLS Variance–Covariance matrix (upper square parenthesis) and the White heteroskedasticity-consistent Variance–Covariance matrix (lower square parenthesis). Figures in bold highlight the rejection of the null hypothesis at the 5% significance level. According to the strong exogeneity criterion, the *STC* core inflation rate is selected as the best core inflation measure, as it is never Granger-caused by the headline inflation rate nor error-correcting relative to the headline inflation rate. *STC* is the only core inflation rate to show this property, as none of the other series passes the joint Granger-causality and error-correction test (Panel C). Moreover, headline inflation is Granger-caused by *STC* and error-correcting; the finding is clear-cut from the joint test.[6]

Moreover, *STC*'s strong exogeneity property also holds relative to the other core inflation measures. *STC* is Granger-causing all the other core inflation measures (Panel A), and all the other core rates error-correct relative to *STC*, apart from PCC2 (Panel B). The joint tests further support this finding, which yields clear-cut evidence of Granger-causality and error-correction forcing from *STC* to the other series. Moreover, none of the variables is Granger-causing *STC*, apart from PCC. *STC* is not error-correcting relative to any other core series (Panel B). The joint Granger-causality and error-correction tests support the above findings, which show only one rejection at the 1% level for PCC.

7.2.1. Additional in-sample forecasting properties

We further assess the ability of the various core inflation measures to track the headline inflation underlying evolution as measured by its centered moving average at various horizons, i.e., from one year (MA12) to five years (MA60). In this respect, the usual benchmark is the centered three-year inflation moving average. In Table 8, Panel A, we report the comparison based on the coefficient of determination from the bivariate prediction regression

$$\pi^s_t = \alpha + \beta\pi^c_t + \varepsilon_t, \tag{35}$$

where $c = SUP, PCC, \ldots, STC$ and $s = MA12, MA24, \ldots, MA60$.

Moreover, in Table 8, Panel B, we report the estimated coefficients in the Mincer-Zarnowitz regressions

$$\pi^s_t = \alpha + \sum_c \beta_c\pi^c_t + \varepsilon_t, \tag{36}$$

where $c = SUP, PCC, \ldots, STC$ and $s = MA12, MA24, \ldots, MA60$. HACSE standard errors are reported for both exercises.

As shown in Panel A, at the three-year horizon, WMED, TR30, and *STC* are the strongest associated measures with smoothed inflation; the others follow closely in the ranking, proving superior to EXFE. At longer horizons, *STC* is best, followed by WMED. At shorter horizons, i.e., at the 1-year or 2-year horizons, TR10 is best. Overall, the findings confirm the association of *STC* with the underlying inflation trend.

Moreover, as shown in Panel B, at the 3-year horizon, *STC* is the only measure retained in the Mincer-Zarnowitz regression (Mincer & Zarnowitz, 1969), while at longer horizons, *STC*, WMED, and TR30 contain valuable information. The evidence is mixed at shorter horizons, yet *STC* is retained in the regression at the 2-year horizon. Overall, *STC* is the best (in-sample) forecaster among the group of core inflation measures at the usual 3-year reference smoothing horizon.

7.2.2. Out-of-sample forecasting properties

In the out-of-sample forecasting exercise, we fix the core inflation forecast at its naive value, i.e., the last in-sample estimate on 2022:8. We compare the AR-12 or non-anchored model

$$\Delta\pi_t = \alpha_1 + \sum_{j=1}^{12}\gamma_{1,j}\Delta\pi_{t-j} + \varepsilon_{1,t} \tag{37}$$

with the ECM(12) or anchored model

$$\Delta\pi_t = \alpha_1 + \sum_{j=1}^{12}\gamma_{1,j}\Delta\pi_{t-j} + \beta_1\left(\pi_{t-1} - \pi^c_{t-1}\right) + \varepsilon_{1,t}. \tag{38}$$

We estimate the models throughout 2022:8. We generate one-step ahead forecasts over the period 2022:9 through 2023–8 without updating parameter estimates. The exercise allows us to assess the future inflation information content of the various core inflation measures and to track the most recent inflation developments. We report the results in Fig. 8. The top plot shows a cross-plot of RMSFE vs. bias (mean forecast error). In this context, the ideal model would be located at the origin, showing zero bias and RMSFE. In the center and bottom plots, we contrast actual and forecasted inflation values for the various models. In particular, in the center plot, we collect the "looser models", i.e., those ranking fourth or lower in the list; in the bottom plot, we collect the

[6] Based on the error-correction test reported in Table 4, Panel B, it appears that headline inflation is error-correcting relative to *STC* at the 10% level only. This result is determined by the wide deviation of headline inflation from *STC* at the end of our sample. For instance, by omitting the last four observations in the sample, the p-value of the t-ratio test for the omission of the error-correction term from the headline inflation equation is [0.0232] (not reported).

Table 8
In-sample forecasting properties for headline HICP inflation centered moving average.

Panel A: *R2* of prediction regressions							
SUP	**PCC**	**PCC2**	**TR10**	**TR30**	**WMED**	**EXFE**	***STC***
0.6	0.77	0.67	**0.89**	0.77	0.72	0.55	0.29
0.51	0.68	0.58	**0.73**	0.69	0.66	0.43	0.39
0.5	0.53	0.53	0.52	0.54	**0.56**	0.42	0.54
0.49	0.41	0.48	0.41	0.45	0.54	0.41	**0.61**
0.46	0.38	0.46	0.33	0.37	0.47	0.36	**0.65**

	Panel B: Mincer-Zarnowitz regressions				
	MA12	**MA24**	**MA36**	**MA48**	**MA60**
SUP	0.434	0.651	0.424	−0.286	−0.082
	(1.79)	**(2.12)**	(1.06)	(−0.67)	(−0.27)
PCC	0.589	0.872	0.320	−0.638	−0.582
	(2.59)	**(2.28)**	(0.69)	(−1.37)	(−1.38)
PCC2	−0.246	−0.913	−0.128	1.682	1.554
	(−0.49)	(−1.34)	(−0.14)	(1.76)	(1.90)
TR10	1.302	0.462	0.079	−0.037	−0.040
	(7.37)	**(2.48)**	(0.34)	(−0.172)	(−0.21)
TR30	−0.335	0.026	−0.134	−0.426	−0.780
	(−1.22)	(0.08)	(−0.34)	(−1.14)	**(−2.39)**
WMED	−0.250	−0.030	0.331	0.979	1.110
	(−1.41)	(−0.16)	(1.48)	**(4.50)**	**(5.28)**
EXFE	−0.474	−0.480	−0.175	0.072	−0.024
	(−3.19)	**(-2.51)**	(−0.68)	(0.271)	(0.13)
STC	0.062	0.309	0.462	0.442	0.506
	(1.09)	**(4.42)**	**(4.98)**	**(4.49)**	**(6.03)**
Const	−0.384	−0.247	−0.360	−0.758	−0.617
	(−1.55)	(−0.74)	(0.43)	(−1.67)	(−1.68)
R2	0.94	0.85	0.76	0.75	0.78

The Table reports the results of the in-sample forecasting analysis. Panel A reports R2 statistics from the prediction regressions of the various core inflation measures relative to the centered moving average of headline inflation. The smoothing period ranges from 1 (MA12) to 5 (MA60) years. Panel B reports the estimated parameters, with HAC *t*-ratios in round brackets, for the Mincer-Zarnowitz regressions of the centered moving averages of headline inflation on the various core rate series. The core inflation series are the Supercore (SUP), the Persistent and Common Component of Inflation (PCC), the Persistent and Common Component of Inflation computed using the Ex-Food and Energy inflation rate (PCC2), the Trimmed Mean inflation rate with 10% and 30% symmetric trimming (TR10, TR30), the Weighted Median inflation rate (WMED), the Ex-Food and Energy inflation rate (EXFE), and the Structural Core rate (*STC*).

"winner models", i.e., those ranking in the first three positions. We also report the AR-12 model forecasts in this latter case for comparison.

The results are clear-cut and confirm out-of-sample the *STC* superior performance established in-sample. *STC* shows virtually zero bias and the lowest RMSFE. *PCCI* and *PCCI*2 follow in the ranking, delivering + 32% and + 65% larger RMSFE, respectively. *PCCI* also shows a bias of about 0.7%. According to the RMSFE, the rest of the ranking is *TR*10 (+78%), *TR*30 (+166%), *SUP* (+184%), *WMED* (+246%), and *EXFE* (+278%). The AR-12 model ranks last (+356%), indicating that a core inflation anchor is essential for in-sample and out-of-sample forecasting. Not surprisingly, the better the core inflation anchor, i.e., the trend measure, the better the forecasting performance. In this respect, *STC* and *PCCI* are the best trackers of the disinflation that started in November 2022 and provide policy-relevant information. Their forecasts for July 2023 were 5.4% and 4.6%, respectively, against an actual HICP inflation value of 5.3%. Yet, both models failed to predict the inflation stabilization in August 2023 (5.3%), yielding 4.8% and 4.1% point forecasts, respectively. The finding is not surprising, given that the relevant past information used in the forecasting regression includes the persistent disinflation since November 2022.

8. Conclusions

This paper introduces a new decomposition of euro area headline inflation into a core or medium to long-term component, a non-core cyclical component, and a residual component related to other short-lived factors. The new core inflation measure, the *structural core inflation* rate, bears the interpretation of expected headline inflation, conditional to medium to long-term demand-side and supply-side developments. Theoretically, it is grounded on Friedman's insights from the quantity theory of money and Eckstein's insights about steady-state inflation and agents' price inflation expectations. In light of its definition and construction, the structural core inflation rate fits with the expected inflation rate component in a textbook Phillip's curve. In addition to theoretical grounding, it shows smoothness and trending properties, economic content, and forecasting ability not only for headline inflation but also for other available measures of core inflation routinely used at the ECB for internal or external communication. It might therefore carry additional helpful information for policy-making decisions. Our measure of cyclical inflation also has valuable information on expected headline inflation, conditional to short-term demand and supply-side developments.

We investigate the source of inflationary pressure within the proposed decomposition since the euro area's inception. Concerning recent developments, the post-pandemic inflationary burst was largely cyclical and driven by both demand-side and supply-side factors. Core inflation also rose through early 2021, driven by supply-side developments partially offset by disinflationary demand-side developments. As core supply-side developments have stabilized since early 2021, core demand-side developments have driven core inflation downward to 3% in 2022. Cyclical headline inflation appears to have lost momentum since June 2022 due to the offsetting impact of cyclical demand-side on cyclical supply-side inflation. In contrast, residual inflation appears to be a persistent source of inflationary pressure in the euro area, coherent with its association with supply-chain and energy price developments and further geopolitical tensions.

Notwithstanding inflationary developments, ECB monetary policy management has successfully mitigated the rise in core inflation, postponing interest rate hikes and preserving macro-financial stability. Currently, cyclical and residual inflations are the most prominent threats to price stability, albeit some evidence of cyclical stabilization can be noted. Yet, although the assessment is preliminary, our results

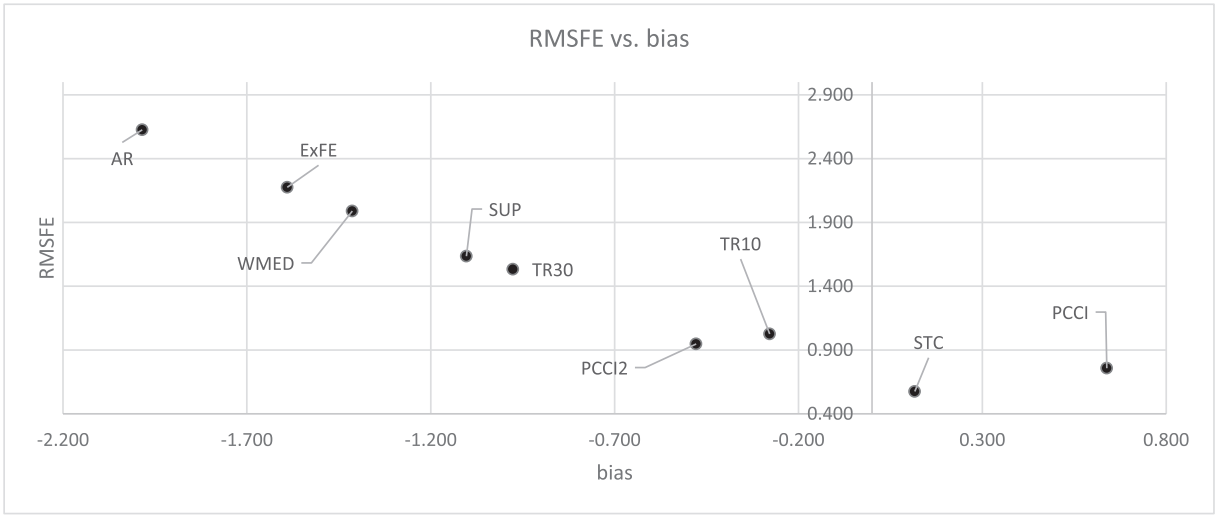

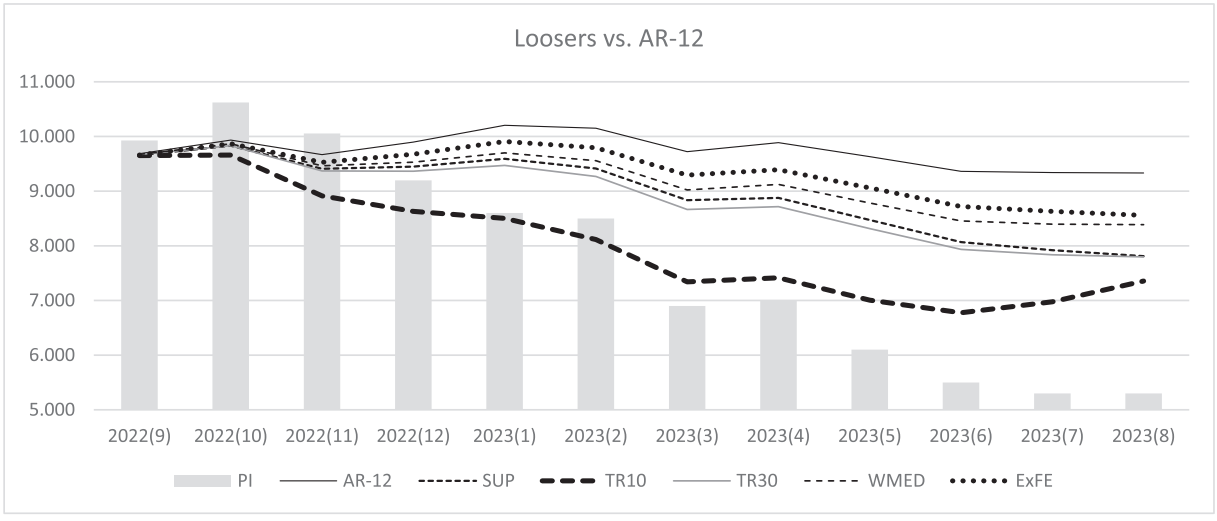

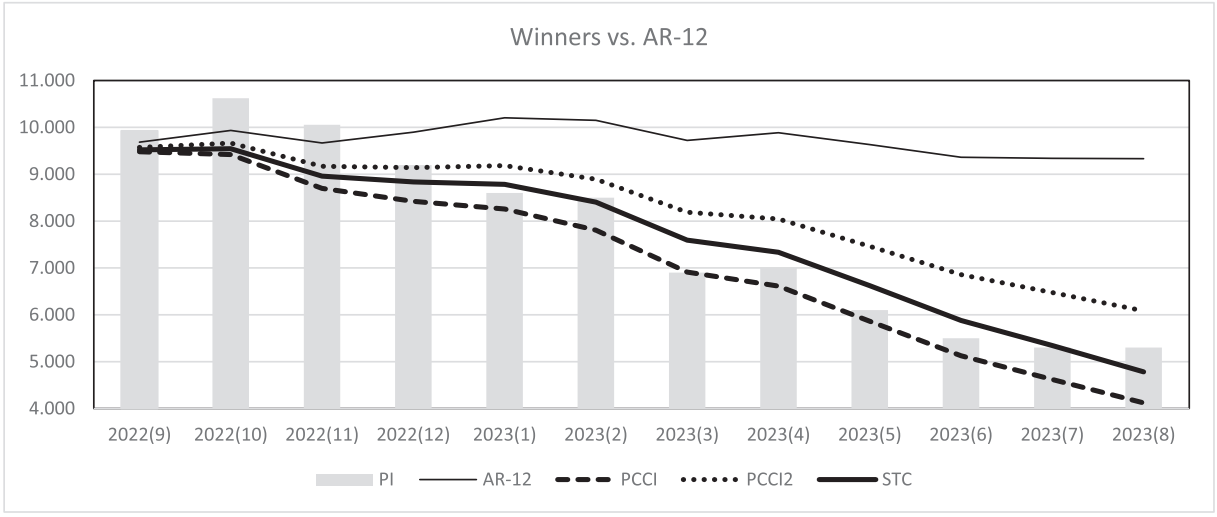

Fig. 8. Out-of-sample inflation forecasts.

indicate a likely weakening of overall financial conditions ahead within an emerging stagflationary scenario. A pressing issue for ECB monetary policy will be to face -mostly supply-side- inflationary pressure without triggering a financial crisis.

9. Appendix 1: Asymptotic properties

Concerning the *MLT-ST* decomposition regression model in (12) in the first step, given data assumptions, the OLS estimator is consistent and asymptotically normal, i.e.,

$$\Upsilon_T(\widehat{\boldsymbol{\theta}} - \theta) \xrightarrow{d} N\left(\mathbf{0}, \sigma^2 \mathbf{Q}^{-1}\right), \tag{39}$$

where

$\theta = \left(\theta_0, \theta_1, \theta_{s,1}, .., \theta_{c,mj^*}\right)$, $\mathbf{Q} = E\left[\mathbf{z}_t^{*'}\mathbf{z}_t^*\right]$, $\mathbf{z}_t^* = \left(1 \quad t \quad \sin(2\pi\frac{t}{T}) \quad \dots \quad \sin\left(2\pi\frac{\sum_{k=1}^{t} x_{1,k}}{\sum_{k=1}^{T} x_{1,k}}\right) \quad \dots\right)'$, and $\underset{(m+2)\times(m+2)}{\Upsilon_T} = diag\left(\sqrt{T}, T^{3/2}, \sqrt{T} \ldots, \sqrt{T}\right)$. See Hamilton (1988; ch. 16); see also Granger and Hallman (1991), Ermini and Granger (1993), and Dittmann and Granger (2002) for stationarity properties of periodic transformations. Supporting Monte Carlo evidence for the *MLT−ST* regression-based decomposition can be found in Morana (2021). Monte Carlo results also show that the methodology is superior to other detrending approaches, such as the HP filter.

Concerning the asymptotic properties of the PC estimator of the common factors $\widehat{\mathbf{f}}$ in (15, 16) in the second step, for $N, T \to \infty$, among other results, Bai (2003) establishes its $min\{\sqrt{N}, \sqrt{T}\}$consistency and asymptotic normality for $\mathbf{f}^0\mathbf{H}$, where $\mathbf{H}$ is an invertible transformation matrix of appropriate order, i.e., for the space spanned by the latent factors. Among other general conditions, this holds under the assumption of I(0) unobserved common factors and idiosyncratic components, where the latter might also display limited heteroskedasticity in both their time-series and cross-sectional dimensions. Since the decomposition in the first step delivers $\sqrt{T}$ consistent estimation of the $\mathbf{n}_t$ and $\mathbf{a}_t$ components, asymptotically, they might be taken as known, and Bai (2003)'s $min\{\sqrt{N}, \sqrt{T}\}$consistency and asymptotic normality of PC estimation of their latent factors can also be conjectured to apply. Supporting Monte Carlo evidence for PCA common factor estimation in a variety of frameworks, including those considered in this study, can be found in Morana (2007),Morana (2014).

Concerning the OLS PC-regression in (17), as noted by Bai (2003), its consistent estimation only requires the consistent estimation of $\mathbf{f}^0\mathbf{H}$. Using $\mathbf{f}^0\mathbf{H}$ as the regressors yields the same predicted value as using $\mathbf{f}^0$. Furthermore, because $\mathbf{f}^0\mathbf{H}$ and $\mathbf{f}^0$ span the same space, testing the significance of $\mathbf{f}^0\mathbf{H}$ is equivalent to testing the significance of $\mathbf{f}^0$. However, inference might require taking into account the estimation error in $\widehat{\mathbf{f}}$. In this respect, Bai (2003) shows that, for $N, T \to \infty$and $\sqrt{T}/N \to 0$, the estimation error can be neglected, i.e., $\mathbf{f}^0$ can be treated as known. Bai and Ng (2006) have further shown that, under the conditions $N, T \to \infty$and $\sqrt{T}/N \to 0$, the OLS estimator of the coefficients in a PC-regression is $\sqrt{T}$ consistent and asymptotically normal. Moreover, the conditional mean predicted by the estimated principal components is $min\{\sqrt{N}, \sqrt{T}\}$consistent and asymptotically normal. Therefore, under the general conditions in Bai (2003) and Bai and Ng (2006), it can be conjectured that

$$\sqrt{T}(\mathrm{vec}(\widehat{\boldsymbol{\Theta}}) - \mathrm{vec}(\Theta)) \xrightarrow{d} N\left(0, \Sigma \otimes E\left[\mathbf{f}_t\mathbf{f}_t'\right]^{-1}\right), \tag{40}$$

i.e., the OLS estimator in (19) is $\sqrt{T}$ consistent and asymptotically normal. In the case of non-spherical residuals, inference on the estimated loadings can be made using Newey-West HACSE.

Empirically, in finite samples the relevance of the estimation error can be assessed by means of unobserved component analysis (Harvey, 1989). For instance, a general model of the form

$$\begin{aligned} y_t &= \mu_t + \gamma_t + \xi_t \\ \xi_t &\sim i.i.d.N\left(0, \sigma_\xi^2\right), \end{aligned} \tag{41}$$

where μ_t is the unobserved trend component (a local level or local trend model), γ_t is the unobserved cyclical or AR component, and ξ_t is the unobserved irregular component, can be set up and estimated by ML and the Kalman filter. The rationale of this specification is to bias the systematic component to be as smooth as possible, i.e., to emphasize potential irregular fluctuations, i.e., observational noise, a priori. The unobserved irregular component provides a measure of the estimation errors, and its magnitude is given by its variance σ_ξ^2, which can the be assessed in relative terms using the inverse signal-to-noise ratio $(s/n)^{-1} = \left[\left(\sigma_\mu^2 + \sigma_\gamma^2\right)/\sigma_\xi^2\right]^{-1}$. The empirical condition $(s/n)^{-1} \to 0$ might then be taken as evidence that the estimation error can be neglected.

10. Appendix 2: Variance decomposition analysis

Given the decomposition in (18) and the orthonormality of the common factors (standardized PCs), the variance decomposition for the vector $\mathbf{y}_t$ is

$$\begin{aligned} \widehat{\boldsymbol{\Sigma}}_{\mathbf{y}} &\equiv \widehat{\boldsymbol{\Theta}}'\widehat{\boldsymbol{\Sigma}}_{\mathbf{f}}\widehat{\boldsymbol{\Theta}} + \widehat{\boldsymbol{\Sigma}}, \\ &\equiv \widehat{\boldsymbol{\Theta}}'\widehat{\boldsymbol{\Theta}} + \widehat{\boldsymbol{\Sigma}} \end{aligned} \tag{42}$$

where $\widehat{\boldsymbol{\Sigma}}_{\mathbf{y}} = \frac{1}{T}\sum_{t=1}^{T}\left(\mathbf{y_t} - \widehat{\boldsymbol{\mu}}_t\right)\left(\mathbf{y}_t - \widehat{\mu}_t\right)'$ and $\widehat{\boldsymbol{\Sigma}}_{\mathbf{f}} = \frac{1}{T}\sum_{t=1}^{T}\widehat{\mathbf{f}}_t\widehat{\mathbf{f}}_t' = \mathbf{I}$.

Hence, considering the generic entry i in the vector $\mathbf{y}_t$, i.e., $\mathbf{y}_{i,t}$, it follows

$$\widehat{\sigma}_{y_i}^2 \equiv \sum_{j=1}^{s+r}\widehat{\Theta}_{i,j}^2 + \widehat{\sigma}_{\varepsilon_i}^2 \tag{43}$$

where $\widehat{\Theta}_{i,j}^2$ is the square of the i,j element in the $\widehat{\boldsymbol{\Theta}}$ loading matrix. The proportion of variance of series y_i accounted by the generic factor k is then $\widehat{\Theta}_{i,k}^2/\widehat{\sigma}_{y_i}^2$.

In the case of non-orthogonal factors, the decomposition in (43) becomes

$$\widehat{\sigma}_{y_i}^2 \equiv \sum_{j=1}^{s+r}\widehat{\Theta}_{i,j}^2 + \sum_{j=1}^{s+r-1}\sum_{q=j+1}^{s+r}\widehat{\Theta}_{i,j}\widehat{\Theta}_{i,q}\widehat{\rho}_{jq} + \widehat{\sigma}_{\varepsilon_i}^2 \tag{44}$$

to account for non-zero sample correlations (or covariances) $\widehat{\rho}_{jq}$ across factors.

In the case the factors were near orthogonal, i.e., some of the sample correlations are non-zero, yet not significant (5% level) $(\widehat{\rho}_{jq}/\sqrt{(1-\widehat{\rho}_{jq}^2)/T-2} < 1.96)$, the decomposition in (43) can still be used, yet only as a (fair) approximation

$$\widehat{\sigma}_{y_i}^2 \simeq \sum_{j=1}^{s+r}\widehat{\Theta}_{i,j}^2 + \widehat{\sigma}_{\varepsilon_i}^2. \tag{45}$$

Otherwise, variance bounds can be constructed. Hence, the proportion of series y_i's variance accounted by the generic factor k is in the range $[\min(a,b), \max(a,b)]$, where $a = \widehat{\Theta}_{i,k}^2/\widehat{\sigma}_{y_i}^2$ and $b = (\widehat{\Theta}_{i,k}^2 + \sum_{q=1,q\neq k}^{s+r}\widehat{\Theta}_{i,k}\widehat{\Theta}_{i,q}\widehat{\rho}_{kq})/\widehat{\sigma}_{y_i}^2$. In practice, in the current context, the case of non-orthogonal factors can arise when the common factors are extracted from transformations of some of the elements in the $\widehat{\mathbf{n}}_t$ or $\widehat{\mathbf{a}}_t$ components. For instance, detrending or first differencing of some of the elements in

the $\hat{\mathbf{n}}_t$ elements might be computed to induce stationarity or enhance the correlation structure and, therefore, the extraction accuracy of the common factors themselves; under this condition, the orthogonality of $\hat{\mathbf{f}}_n$ and $\hat{\mathbf{f}}_a$ is not granted any longer, as it holds by construction for the untransformed $\hat{\mathbf{n}}_t$ and $\hat{\mathbf{a}}_t$ components. See also Brusco, Singh, and Steinley (2009) about heuristic tools to decide the optimal set of variables for PCA analysis concerning variable inclusion (and transformation).

Declaration of Competing Interest

The authors declare that they have no known competing financial interests or personal relationships that could have appeared to influence the work reported in this paper.

Acknowledgments

The paper was partially written while the author was Visiting Fellow at the Minda de Gunzburg Center for European Studies at Harvard University. The paper was presented at the New Research on Europe Seminar Series at the Minda de Gunzburg Center for European Studies (Harvard University), the Research Seminar Series (Prague University of Economics and Business), the Midwest Econometrics Group (MEG) 2022 Conference (Michigan State University), the 2022 Computational Financial Econometrics Conference (King's College), the 8th CefES International Workshop: Europe in Unchartered Waters (University of Milano-Bicocca), the RCEA-Europe International Conference on Global Threats to the Global Economy (University of Milano-Bicocca), the 19th EUROFRAME Conference on Economic Policy Issues in Europe. The Return of Inflation: Challenges for European Economies (Sciences Po), the 5th International Conference on European Studies (KOF-ETH), the IAAE 2023 Annual Conference (Norwegian Business School), the EcoMod2023 International Conference on Economic Modeling and Data Science (Czech University of Life Sciences), the European Central Bank Conference on Inflation: Drivers and Dynamics 2023 (ECB), the 54th Annual Conference of the Money, Macro and Finance Society (University of Portsmouth). The author thanks F.C. Bagliano, N. Cassola, H-H Kotz, the reviewers, and seminar and conference participants for constructive comments.

Appendix A. Supplementary data

Supplementary data associated with this article can be found, in the online version, athttps://doi.org/10.1016/j.resglo.2023.100159.

References

Bagliano, F. C., & Morana, C. (1999). Measuring core inflation in Italy. *Giornale degli Economisti, 58*, 301–328.
Bagliano, F. C., Golinelli, R., & Morana, C. (2002). Core inflation in the euro area. *Applied Economics Letters, 9*, 353–357.
Bagliano, F. C., & Morana, C. (2003). Measuring U.S. core inflation: a Common Trends approach. *Journal of Macroeconomics, 25*, 197–212.
Bagliano, F. C., & Morana, C. (2017). It ain't over till it's over: A global perspective on the Great Moderation Great Recession interconnection. *Applied Economics, 49*, 4946–4969.
Bai, J. (2003). Inferential theory for factor models of large dimensions. *Econometrica, 71*, 135–171.
Bai, J., & Ng, S. (2006). Confidence intervals for diffusion index forecasts and inference for factor-augmented regressions. *Econometrica, 74*, 1133–1150.
Ball, L., & Mazumder, S. (2021). A Phillips curve for the euro area. *International Finance, 24*, 2–17.
Bańbura, M., & Bobeica, E. (2020). *PCCI – a data-rich measure of underlying inflation in the euro area* (p. 38). No: ECB Statistics Paper Series.
Beaudry, P., Galizia, D., & Portier, F. (2020). Putting the cycle back into business cycle analysis. *American Economic Review, 110*, 1–47.
Blinder, A. S. (1982). The anatomy of double-digit inflation in the 1970s. In R. E. Hall (Ed.), *Inflation: Causes and Effects* (pp. 261–282). Chicago: University of Chicago Press.
Bobeica, E., & Jarocinski, M. (2019). Missing disinflation and missing inflation: A VAR perspective. *International Journal of Central Banking, 15*, 199–232.
Borio, C. (2014). The financial cycle and macroeconomics: what have we learnt? *Journal of Banking and Finance, 45*, 182–198.
Borio, C., Drehmann, M., & Xia, D. (2019). Predicting recessions: financial cycle versus term spread. *BIS Working Papers, No. 818*.
Borio, C., 2022. Inflation: a look under the hood. In BIS Annual Economic Report. June 2022, 41–73.
Brusco, M. J., Singh, R., & Steinley, D. (2009). Variable neighborhood search heuristics for selecting a subset of variables in principal component analysis. *Psychometrika, 74*, 705–726.
Bryan, M. F., & Cecchetti, S. G. (1994). Measuring core inflation. In N. G. Mankiw (Ed.), *Monetary Policy*. Chicago: University of Chicago Press.
Castle, J. L., Doornik, J. A., & Hendry, D. F. (2021). Robust discovery of regression models. *Econometrics and Statistics*. https://doi.org/10.1016/j.ecosta.2021.05.004. forthcoming. Available at.
Chan, J. C., Clark, T. E., & Koop, G. (2018). A new model of inflation, trend inflation, and long-run inflation expectations. *Journal of Money, Credit and Banking, 50*, 5–53.
Cochrane, J. H. (2022). *The Fiscal Theory of the Price Level*. Princeton University Press.
Cristadoro, R., Forni, M., Reichlin, L., & Veronese, G. (2005). A core inflation indicator for the Euro Area. *Journal of Money, Credit, and Banking, 37*, 539–560.
Dittmann, I., & Granger, C. W. J. (2002). Properties of nonlinear transformations of fractionally integrated processes. *Journal of Econometrics, 110*, 113–133.
Eckstein, O. (1981). *Core Inflation*. New York: Prentice Hall.
Ehrmann, M., Ferrucci, G., Lenza, M., & O'Brien, D. (2018). Measures of underlying inflation for the euro area. ECB. *Economic Bulletin, 4*.
Ermini, L., & Granger, C. W. J. (1993). Some generalizations on the algebra of I(1) processes. *Journal of Econometrics, 59*, 369–384.
Freeman, D. G. (1998). Do core inflation measures help forecast inflation? *Economics Letters, 58*, 143–147.
Friedman, M., 1969. The Optimal Quantity of Money and Other Essays. Chicago: Aldine Publishing Company, 1969.
Fröhling, A. Lommatzsch, K., 2011. Output sensitivity of inflation in the euro area: indirect evidence from disaggregated consumer prices. Deutsche Bundesbank Discussion Paper Series 1: Economic Studies, No. 25.
Granger, C. W. J., & Hallman, J. (1991). Nonlinear transformations of integrated time-series. *Journal of Time Series Analysis, 12*, 207–224.
Gordon, R. (1975). Alternative responses of policy to external supply shocks. *Brookings Papers on Economic Activity, 1*, 183–206.
Goodhart, C., & Pradhan, M. (2020). *The Great Demographic Reversal: Ageing Societies, Waning Inequality, and an Inflation Revival*. London, UK: Palgrave Macmillan.
Hamilton, J. D. (1994). *Time Series Analysis*. Princeton University Press.
Hasenzagl, T., Pellegrino, F., Reichlin, L., & Ricco, G. (2022). A Model of the Fed's view on inflation. *The Review of Economics and Statistics, 104*, 686–704.
Hodrick, R. J., & Prescott, E. C. (1997). Postwar US business cycles: an empirical investigation. *Journal of Money, Credit, and Banking, 29*, 1–16.
Jarocinski, M., & Lenza, M. (2018). An inflation-predicting measure of the output gap in the euro area. *Journal of Money, Credit and Banking, 50*, 1189–1224.
Kishor, N. K., & Koenig, E. F. (2022). Finding a role for slack in real-time inflation forecasting. *International Journal of Central Banking, 18*, 245–282.
Lane, P. R. (2022). *Inflation Diagnostics*. The ECB Blog.
Martens, E. (2016). Measuring the level and uncertainty of trend inflation. *The Review of Economics and Statistics, 98*, 950–967.
Mincer, J., & Zarnowitz, V. (1969). *The evaluation of economic forecats. Economic Forecasts and Expectations: Analysis of Forecasting Behavior and Performance, 3–46*. National Bureau of Economic Research.
Morana, C. (2002). Common persistent factors in inflation and excess nominal money growth and a new measure of core inflation. *Studies in Non Linear Dynamics and Econometrics, 6*(3), art.3.
Morana, C. (2007). A structural common factor approach to core inflation estimation and forecasting. *Applied Economics Letters, 14*, 163–169.
Morana, C. (2007). Multivariate modelling of long memory processes with common components. *Computational Statistics and Data Analysis, 52*, 919–934.
Morana, C. (2014). Factor vector autoregressive estimation of heteroskedastic persistent and nonpersistent processes subject to structural breaks. *Open Journal of Statistics, 4*, 292–312.
Morana, C. (2021). A New Macro-financial condition index for the euro area. *Econometrics and Statistics*. in press.
Nickel, C., Koester, G., & Lis, E. (2022). Inflation developments in the euro area since the onset of the pandemic. *Intereconomics, 57*, 69–75.
Quah, D., & Vahey, S. P. (1995). Measuring core inflation. *Economic Journal, 105*, 1130–1144.
Roubini, N., 2022a. From Great Moderation to Great Stagflation. Project Syndicate. Aug 9, 2022.
Roubini, N., 2022b. The Stagflationary Debt Crisis is Here. Project Syndicate. Oct 3, 2022.
Spence, M., 2022. Secular Inflation. Project Syndicate, Oct 12, 2022.
Svensson, L. E. (1997). Inflation forecast targeting: Implementing and monitoring inflation targets. *European Economic Review, 47*, 1111–1147.
Wynne, M. A. (2008). Core inflation: A review of some conceptual issues. Federal Reserve Bank of St. *Louis Review, 90*, 205–228.